Catalysis Today xxx (xxxx) xxx

Contents lists available at ScienceDirect

Catalysis Today

journal homepage: www.elsevier.com/locate/cattod

Review on covalent organic frameworks and derivatives for electrochemical and photocatalytic CO_2 reduction

Zizhou He [a,1], Joshua Goulas [a,1], Evana Parker [a], Yingqiang Sun [b], Xiao-dong Zhou [a,*], Ling Fei [a,*]

[a] Department of Chemical Engineering, Institute for Materials Research and Innovations, University of Louisiana at Lafayette, Lafayette, LA 70504, USA
[b] School of Chemistry and Chemical Engineering, Anhui University, Jiulong Road 111, Anhui 23003, China

ARTICLE INFO

Keywords:
COFs
CO_2 reduction
Electrochemical
Photocatalytic
Catalysis

ABSTRACT

With increasing potential for environmental volatility in the wake of increasing atmospheric pollutants, the need for sustainable approaches towards renewable energy and pollution reduction is ever-expanding. In recent years, research has geared towards utilizing carbon dioxide, which is seen as the largest threat of climate change, to produce various other useful chemicals while decreasing carbon dioxide levels. Considering this recent research, covalent organic frameworks (COFs) have jumped into the spotlight as promising and exciting new catalysts development to drive efforts towards easing climate change. As a relatively new class of materials, COFs are high surface area crystalline networks with a large degree of fine-tunable chemistry and the capability of metallic hybridization and functional group modifications. This review is a comprehensive and detailed discussion of the recent research accomplishments and goals of both photocatalytic and electrocatalytic carbon dioxide reduction using COFs as catalysts. Recent COF electrochemical catalysis is thoroughly discussed through different metal-based and pristine COFs along with the material design principles necessary to reduce carbon dioxide effectively and selectively. COF photocatalysis is discussed namely on the remarkable ability of irradiation-induced carbon dioxide reduction for pristine metal-free, metalated, and hybrid COFs along with the ability of photo-coupled electrocatalytic reduction. Additionally, final conclusions on the state of COF research are provided along with future suggestions towards expanding and improving the investigation and application of COFs for CO_2 reduction.

1. Introduction

Millions of tons of CO_2 emission resulting from fossil fuel-driven economy, have significantly affected the ecosystems on earth and led to severe environmental issues. Additionally, with global industrialization and urbanization, the demand for energy sources has been continuously on the rise [1]. Under this scenario, the conversion of CO_2 to value-added fuels and chemicals has been considered a promising strategy to mitigate global warming and energy supply problems in a long run. Thus, electrochemical and photocatalytic CO_2 reduction has received tremendous attention in the past decade.

Nevertheless, in order to achieve CO_2 conversion of high efficiency and selectivity, the design and development of tunable, highly efficient, and stable catalysts are pivotal. All catalysis processes involve mass transport that transfers reactants or products in and out of catalytically active sites. Porous materials are therefore essential to ensure abundant active sites with easy access. In this regard, Metal-Organic Frameworks (MOFs) first developed in 1990 s and its derivatives (e.g. porous carbon via thermal treatment) have been intensively studied and demonstrated great promise in CO_2 reduction, owing to their great flexibility and control on pore size, geometry, and active metal loading [2]. Due to the popularity of MOFs, several insightful reviews on MOFs for CO_2 capture or conversion have been available [2–6].

Noteworthy, Covalent Organic Frameworks (COFs), discovered in 2005 (roughly one decade later than MOFs), share many similarities and advantages with MOFs. COFs have recently emerged into a prominent family of CO_2 reduction materials, though the research is still at the infancy stage. Thus, it is of great interest to have a dedicated review on COFs to summarize the recent progress on CO_2 reductions and offer perspectives on the future directions. First, COFs will be introduced and compared with MOFs in terms of properties and control over materials design. Afterwards, the COFs and its derivatives for CO_2 will be

* Corresponding author.
E-mail addresses: xiao-dong.zhou@louisiana.edu (X.-d. Zhou), ling.fei@louisiana.edu (L. Fei).
[1] These authors contributed equally to the work.

https://doi.org/10.1016/j.cattod.2022.04.021
Received 31 January 2022; Received in revised form 11 April 2022; Accepted 18 April 2022
Available online 26 April 2022

categorized into electrochemical and photocatalytic catalysis with representative examples included. Insights for future research into COF materials are provided at the end. There are a few excellent reviews on COFs' chemistry and applications [1,7–10]. This review is based on material science and engineering perspectives of works up to year 2022, which can serve as a great complementary summary to currently available reviews.

2. COFs

2.1. Properties

COFs are a class of crystalline porous materials that share great similarities with MOFs including flexible structural pre-designability, periodic porosity, and highly ordered structures. The key difference between MOFs and COFs lies on the fundamental chemistry of synthesis. MOFs are based on inorganic coordination chemistry involving organic linker and inorganic metal ion centers, while COFs are entirely built from organic building block molecules (monomers) connected by covalent bonds [8]. Because of high strength of covalent bonds, COFs have better thermal and chemical stability than MOFs [11]. During the polymerization, bond connection is spatially confined at either a two- or three-dimensional (2D or 3D) way or geometrically guided to produce extensive and highly ordered 2D or 3D porous architecture [12]. The building blocks, namely monomers, have a very diverse pool of selection, thereby, form COFs of various structure and porosity. Functional groups or metal ion coordination can be either present already in the linker molecules or introduced to COF via post-modification. Additionally, heteroatoms can be easily introduced (e.g. triazines and imines) to COFs to provide special microenvironments or serve as binding sites for metals or redox-active sites [9]. Different from MOFs, many COFs have extensive π-conjugated structures and show a modest electronic conductivity, making them promising candidates for catalysis. With templates or different processing techniques (e.g. 3D print), COFs structure at macroscopic level can be tuned [13,14]. Beyond pristine COFs, metal sites or other materials can be incorporated to form functional composite materials. Meanwhile, highly ordered nanostructured porous carbon materials, or carbon-metal based composite materials can be

Table 1
The COF synthesis approaches and their characteristics [16].

Method		Organic solvents	Operating conditions			Product			Advantage	Disadvantage
			Temperature (°C)	Time (h)	Pressure	Yield (%)	S_{BET} (m^2/g)	Morphology		
Solvothermal synthesis		Abundant	70–150	~72	Degassing and seal	70–95	500–3000	Powder	Widely used	Organic solvents; Heating
Mixed solvent-based synthesis		~50%	RT/140	24–48	ATM	47–89	100–1300	Powder	Better crystallinity	Reduced but still relatively abundant solvent
Solid phase synthesis	Mechano-chemistry	No or a few drops	RT	1–2	ATM	85–90	~100	Powder	No or very little organic solvents; Large-scale synthesis; Synthesis of some uncommon COFs	Moderate crystallinity; Limited applications
	Mechano-chemistry + thermal crystallization	No or a few drops	70–150	1–120	ATM/ Degassing and seal	75–90	300–3000	Powder /Various shapes	Improved crystallinity compared to mechanochemistry	Use of organic solvents and heating in crystallization step
	Solvent-free directing heating	No	80	72	Seal	83	296	Powder	Solvent-free; Catalyst-free	One precursor is liquid
	Electron beam irradiation approach	A certain amount	RT	160 s	Degassing and seal	92	738	Powder	Energy-saving; Ultrarapid	Reaction conditions need to be critically controlled
Vapor-assisted approach		A little	RT/120	48–72	ATM	~85	280–1000	Powder/ Film	very little organic solvents; COF film can be obtained	Moderate crystallinity (powder) Lower yield (film)
Ionothermal synthesis		No	RT to 140	~72	ATM/ Degassing and seal	70–95	400–1300	Powder	Recyclable; No organic solvent; Safe; Functionalized modification to COFs	High cost
Hydrothermal synthesis		No	RT/120	0.5–72	ATM/ Degassing and seal	70–97	300–1500	Powder /Colloid	Water as solvent; Large-scale synthesis	Limited application range
Micelle-assisted synthesis		A little	30	72	Deoxygenation	86–93	687	Sub-20 nm particles	Synthesis of uniform nanometer-sized COF particles	Reaction conditions need to be carefully optimized

(RT: room temperature; ATM: atmospheric pressure; S_{BET}: BET surface area)

derived from COFs via synthetic processes like pyrolysis. Overall, COFs represent an emerging class of materials that will advance fundamental understanding and applications.

2.2. Synthesis methods

The most frequently applied synthesis strategy for COFs is the solvothermal method. In a typical process, a Pyrex tube of desired volume is charged with reactant monomers, catalysts, and solvents. After sonication for a certain period to disperse the mixture evenly, the tube was flash-frozen and degassed by several freeze-pump-thaw cycles through the pump and then sealed under vacuum. The sealed tube is maintained at a suitable temperature for synthesis reaction for required time period. Afterwards, the product precipitates will be collected via filtration or centrifugation and washed with one or more appropriate solvents before vacuum drying. Sometimes, Soxhlet extraction is used to exchange solvents or remove impurities [8,15]. Finally, the product will be vacuum dried between 80 and 120 °C for hours. As can be seen, these current methods often involve the use of large amounts of organic solvents and have very tedious preparation procedures. In recent years, effort has been extended to exploring facile and green methods. New methods reported include microwave synthesis, ionothermal synthesis, solid phase synthesis, and interface synthesis. Thanks to an excellent recent review on COFs green synthesis, no deep dive into the synthesis part will be attempted in this review. The table summarizes the COF synthesis approaches and their characteristics is cited here for the reader's convenience [16]. Table 1.

3. Electrochemical CO_2 reduction

In recent years, the electrochemical reduction of CO_2 has attracted lots of interest due to the following advantages: the product is controllable with electro-potential; cheap and environmentally friendly solvents or water as reaction medium; the reactor can be scaled up for practical application; the reaction can be powered by renewable energy without extra CO_2 emission [17–20]. However, the practical application is still limited by the poor catalytic activity and insufficient stability [21,22]. COFs with the advantages of being precisely designable at the molecular level, tunable pores and porosities, excellent stability, and π-conjugated structures are considered to be ideal platforms for CO_2 reduction reaction (CO_2RR) [23,24]. In this section, the development and progress of COFs catalyst for CO_2 electrochemical reduction is summarized and discussed.

3.1. Co-based COF catalyst

Co-based material is one of the most extensively studied materials for electrochemical reduction of CO_2 [25], and Co-based COFs have been at the forefront of the emerging COF-based CO_2RR catalysts due to their high activity and selectivity. COF catalysts for CO_2RR were first carried out by Lin et al. in 2015 [26]. In this pioneering work, COF-366-Co in Fig. 1a was first prepared as a model framework by the imine condensation of 5,10,15,20-tetrakis(4-aminophenyl) porphinato]cobalt [Co (TAP)] with 1,4-benzenedicarboxaldehyde (BDA). With a rectangular rod-shaped morphology (Fig. 1b), it has a BET (Brunauer-Emmett--Teller) surface area of 1360 m^2/g with a narrow pore size distribution (10–18 Å). When deposited on porous, conductive carbon fabric for electrochemical experiments, the COF-366-Co demonstrated a prominent catalytic effect on the reduction of CO_2 to CO in neutral aqueous solution, reaching Faradaic efficiency FE_{CO}= 90% at an optimal potential of − 0.67 V (vs. reversible hydrogen electrode (RHE)), yielding more than 36 mL mg^{-1} of CO over 24 h. Taking advantage of the design flexibility of the reticular COF platform, the authors further expanded the pore size of the COF-366-Co by replacing BDA with biphenyl- 4,

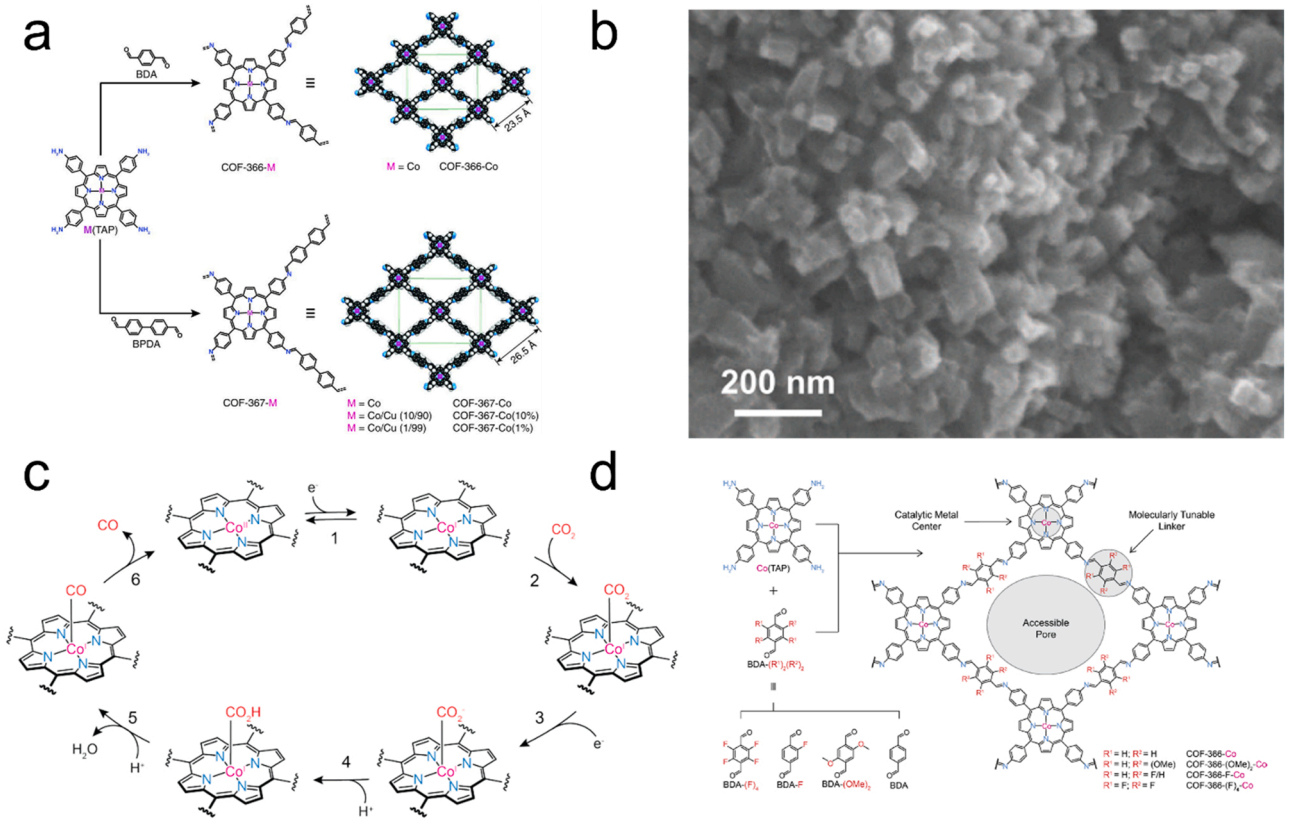

Fig. 1. a) Design and synthesis of metalloporphyrin-based COFs for CO_2 reduction; b) SEM (scanning electron microscope) of COF-366-Co;[26] c) Proposed mechanism for electrocatalytic CO_2 reduction in COF-366-Co; d)Design and synthesis of cobalt-porphyrin-derived COFs for CO_2 reduction [27].

4′-dicarboxaldehyde (BPDA) to form COF-367-Co (Fig. 1a). COF-367-Co not only shares analogous constitution and topology to that of COF-366-Co, but also shows an increase in channel width (24 Å), BET surface area (1470 m^2/g) and pore size distribution (12–23 Å). The expanded framework showed 2.2 times greater enhancement of catalytic current at the identical potential of − 0.67 V of COF-366-Co, yielding more than 100 mL mg^{-1} of CO over 24 h with higher FE_{CO}= 91%. The improved performance of COF-367-Co indicated that the expanded framework could offer a higher CO_2 adsorption capacity and more efficient exposure of the electroactive sites to the reactants. Afterwards, the authors diluted Co-active sites of COF-367-Co to maximize the utilization ratio of active metal sites by introducing inactive copper porphyrin units in the framework to form bimetallic COF-367 derivatives, denoted as COF-367-Co (10%) and COF-367-Co (1%). The percentage indicates the ratio of cobalt in full metal sites. The COF-367-Co (1%) achieved turnover number per electroactive cobalt $TON_{EA} \approx 296{,}000$, indicating its high efficiency of electrochemical CO_2 reduction.

Following this pioneering research, the same research group further optimized COF-366-Co material with different electron-withdrawing groups to realize electronic communication between reticulated metal centers and the surrounding linkages. This enabled reticular electronic tuning of the catalytically active sites, consequently, their catalytic reactivity [27]. The mechanism of CO_2 reduction with COF-366-Co is shown in Fig. 1c, in the first step Co(II) reduced to Co(I), Co(I) is known as the active site for CO_2 reduction. Inspired by the finding that electron-withdrawing groups can promote the Co(II)/Co(I) redox transition, a group of COFs with different electron-withdrawing groups on their respective struts were prepared, including COF-366-Co, COF-366-$(OMe)_2$-Co, COF-366-F-Co, and COF-366-$(F)_4$-Co, as shown in Fig. 1d. The cobalt L-edge X-ray absorption spectroscopy (XAS) data of the functionalized COFs were obtained to study the inductive effects of the reticular structure. According to the XAS analysis, the electron-withdrawing effect of the linking units on the cobalt active center was determined in the following order: COF-366--Co<COF-366-$(OMe)_2$-Co<COF-366-F-Co<COF-366-$(F)_4$-Co. This result confirms that functionalization of the struts with electronegative elements lead to an electron-withdrawing effect on the cobalt center and the extent of this effect is proportional to the electronegativity, as well as the number of functional groups incorporated. The performance enhancement of the electron-withdrawing effect in catalysis was observed for all except COF-366-$(F)_4$-Co. The low activity of COF-366-$(F)_4$-Co could be ascribed to its higher hydrophobicity that restricts the access of electrolytes. This study exemplified the direct electronic structure-function relationships, providing more strategy for COF catalysts design.

Unsatisfying conductivity is the main barrier of COF catalysts [28]. Constructing an orient electron transmission pathway with an electron donor and acceptor has been realized as an effective way to enhance the electron transfer efficiency for CO_2RR reduction [29,30]. An and co-workers integrated crown ethers into Co-porphyrin to form TAPP (Co)-(B18C6-COF) [31]. Crown ethers have a strong binding ability with inorganic or organic guests, owing to their cyclic cavities and electron-donating properties. The introduction of crown ether units not only significantly promoted hydrophilicity with a water contact angle of 58.7° (92° for COF-366-Co), but also enhanced the conductivity to 7.2×10^{-8} S m^{-1} (10 folds of COF-366-Co), resulting in 90.5% FE_{CO} and 1267 h^{-1} turnover frequency (TOF) at −0.9 V. Moreover, Cao's group synthesized cobalt-porphyrin-based COF catalysts containing donor-acceptor (D-A) heterojunctions using sulfur-containing thieno[3, 2-b] thiophene-2,5-dicarbaldehyde (TT) and tetrathiafulvalene (TTF) struts to react with 5,10,15,20-tetrakis(4-aminophenyl)-porphinatocobalt (Co-TAPP), forming TT-Por(Co)-COF and TTF-Por(Co)-COF, respectively [32,33]. In the case of TT-Por(Co)-COF, sulfur-containing aromatic heterocycles and their derivatives, serve as a class of excellent electron donors with high electron mobility, which can enable highly conductive charge transfer materials when being combined with molecules as electron acceptors [33]. Similarly, TTF is an excellent electron donor capable of rapid electron transfer for TTF-Por(Co)-COF, and thus improving the overall electron-transfer efficiency [32]. The TT and TTF incorporation exhibit 2 and 20-fold enhancement of conductivity and 3 and 4 times greater carrier mobility than those of COF-366-Co, respectively. Their favorable charge transfer capability made them outperform COF-366-Co in CO_2RR catalysis. In detail, TT-Por(Co)-COF nanosheets showed high Faradaic efficiency of CO (91.4%, −0.6 V vs. RHE) and a partial current density of 7.28 mA cm^{-2} at −0.7 V versus RHE in an aqueous solution. TTF-Por(Co)-COF has CO_2RR performance in water with 95% Faradaic efficiency of the CO_2-to-CO conversion at −0.7 V vs. RHE and a partial current density of 6.88 mA cm^{-2} at −0.9 V vs. RHE. In addition, other strategies like introducing different metal sites on linking units, integrating the COFs with conductive substrates, also demonstrated significant potential to enhance conductivity [28,34,35]. For instance, Lu et al. reported template-oriented polymerization of covalent organic frameworks (COFs) with isolated cobalt porphyrin units on amino-functionalized carbon nanotubes for efficient electrocatalytic CO_2 reduction reaction (CO_2RR). Compared with pure COFs, the composite materials with ultrathin COF nanolayers wrapped on the conductive scaffold leads to high current density and stable Faradaic efficiency for CO_2-to-CO conversion over a wide potential range [35].

Metallophthalocyanines with excellent molecular electrocatalytic performance mounted into the COFs towards CO_2RR were also explored recently [15,36,37]. Jiang's group developed a CoPc-PDQ-COF catalyst (Fig. 2a and b), by connecting phenazine linkage with metallophthalocyanine catalytic sites into a π-conjugated lattice, exhibiting a FE of 96% with an exceptional TON up to 320,000 and a long-term TOF of 11,412 h^{-1}, indicating a 32-fold increment compared to molecular catalyst [36]. The XRD results of CoPc-PDQ-COF catalyst after 40 days treatment in different solvents confirmed its excellent chemical and thermal stabilities (Fig. 2c). It also shows exceptional bulk conductivity (3.68×10^{-3} S m^{-1}). It is concluded the phenazine linkage endows the framework with high stability and conductivity, while the metallophthalocyanines offer the electrocatalytic sites for CO_2RR. Similar advantages are observed in other metallophthalocyanine-based COF catalysts [15,37].

3.2. Other metal-based COF catalyst

Considering the scarcity of the cobalt resource, earth-abundant alternatives were explored. Bandomo et al. reported the first Mn-based COF (COF_{bpyMn}) by loading single-atom centers, {fac-Mn$(CO)_3$S}, (S = Br, CH_3CN, H_2O), within a bipyridyl based COF, denoted COF_{bpyMn} (Fig. 3a). The catalyst showed low CO_2RR onset potential (η = 190 mV), high current densities(> 12 mA·cm^{-2}, at 550 mV overpotential), as well as good selectivity (up to 72% versus H_2) [38]. More importantly, this work highlighted the crucial role of COF structures in preventing the formation of undesired intermediate (Mn^0–Mn^0 dimers), which is generally observed in molecular Mn-based catalysts. In detail, molecular Mn(I) complexes tend to form Mn^0–Mn^0 dimers, which cannot effectively reduce CO_2. To understand the absence of dimers in the COF_{bpyMn}, the authors studied the dimerization process within the framework via DFT (density-functional theory) calculation (Fig. 3b). They first constructed the COF model structure (COF_{bpyMn}2-A) by anchoring the Mn atoms and rotating the COF layers. The DFT energies results show the COF stabilized the Mn reactants (A1) with bpy ligands in nearby layers (Fig. 3c) and destabilized the Mn dimers (A3) by the mechanical constrains from the stacking pattern of the COF. Taken together, experimental ATR-IR-SEC (attenuated-total-reflection infrared spectroelectrochemical) and computational DFT data, Fig. 3d present the proposed mechanism. As can be seen, the initial reduction at −1.25 V vs SCE results in the loss of Br anion and solvent replacement around the isolated Mn centers. The 50 mV difference compared with molecular catalyst (−1.3 V vs SCE) can be attributed to the electron

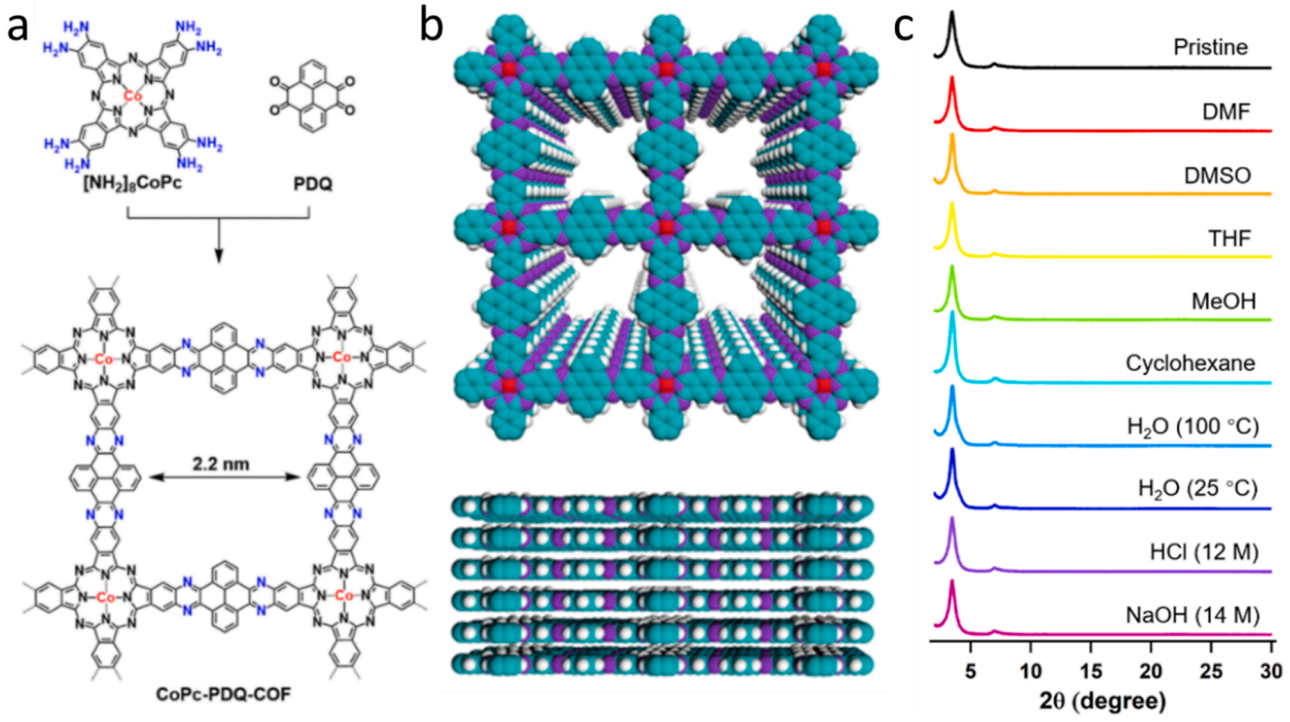

Fig. 2. a) Synthesis of CoPc-PDQ-COF catalyst; b) Top and side view of CoPc-PDQ-COF;c) XRD patterns of CoPc-PDQ-COF after 40 days treatment in different solvents [36].

delocalization of the COF structure, indicating the COF structure can facilitate the initial reduction process. There are no Mn^0−Mn^0 dimers observed in the experimental which supports the computational models. Main catalytically active species [Mn^{-I}] for CO_2 reduction were detected after the reduction. In summary, the COF structure mechanically constrained the Mn active sites and bypassed the dimer formation, resulting in reduced overpotential and enhanced overall catalytic performance. In addition to Mn, other transition metal-based COFs were also investigated. Kubiak's group reported a Fe-based COF, containing 5,10,15, 20-tetra-(4-aminophenyl)-porphyrin Fe (III) chloride (FeTAPPCl) and 2,5-dihydroxyterephthalaldehyde (Dha), for the reduction of CO_2 to CO via a solvent-free method. The Iron porphyrin-based COF catalyst demonstrates a good catalytic activity for CO_2 reduction to CO, with a TOF ($> 600\ h^{-1}\ mol^{-1}$ of Fe) and average FE_{CO}= 80% at −2.2 V (vs. Ag/AgCl) over 3 h in MeCN with 0.5 M trifluoroethanol. Surface XPS (X-ray photoelectron spectroscopy) and ICP-OES (inductively coupled plasma optical emission spectroscopy) studies confirmed the COF is highly stable throughout the catalytic process and conditions [39]. A Cu-based COF was developed via solvothermal method followed by post-modification with 2,4-diamino-6-cholo-1,3,5-triazine (denoted as Dct) [40]. Dct acts as functionalizing exfoliation agent to simultaneously modify and exfoliate COF into large-scale (~ 1.0 mm) and ultrathin (~ 3.8 nm) nanosheets (Cu-Tph-COF-Dct). The Cu-based catalyst exhibited good performance with FE = 80% of CH_4 and a current density of 220.0 mA cm^{-2} at −0.9 V. The Dct functionalized group is revealed to enhance the absorption/activation of the CO_2 near the active sites, stabilize intermediates, and facilitate the generation of CO to enrich the CO concentration around the Cu active sites. In turn, it enhanced catalytic activity towards CH_4 production. Su et al. found covalent triazine frameworks (CTF, a subclass of COF) can act as a great platform to bond coordinatively unsaturated metal species (Co, Ni, Cu) for CO_2RR. Because CTF allows to precisely tune the adsorption energies of critical intermediate species via modulating the coordination number of active centers. Compared with the control sample that has tetraphenylporphyrin (TPP) coordinated Ni, the performance of Ni-CTF is much higher. Overall, these different COFs based catalysts demonstrate great promise of COFs for CO_2RR [41].

3.3. *Pristine COFs: Metal-free catalyst*

Metal-free catalysts are a promising class of catalysts, featuring intriguing advantages in aqueous electrochemical reactions owing to low cost, tunable chemical/electronic structures, and high tolerance to acidic/alkaline conditions [42,43]. Metal-free COF for CO_2RR were also explored recently [44–47]. A series of CTF catalysts with tunable surface functionality by introducing a variety of heteroatom doping (F, Cl, N) were reported for CO_2RR [45]. The primary perfluorinated covalent triazine framework (FN-CTF-400) was prepared by one-step polymerization of tetrafluoroterephthalonitrile with the ionothermal assistance of molten $ZnCl_2$ at 400 °C, as shown in Fig. 4a. The FN-CTF-400 with substantial F-covalent functions as a highly selective electrocatalyst for the conversion of CO_2 to CH_4 with a FE_{CH4}≈ 100% at −0.8 V (Fig. 4b) [45]. DFT calculations (Fig. 4c) were applied to study the role of different heteroatom doping towards the selectivity. Top views of the heteroatom doping structure and the DFT calculated reaction free energy diagram (FED) of the active sites for CO_2 electroreduction were presented. As the FED results shown, edge-gN and edge-2gN are the catalytic sites for the samples responsible to produce CO and CH_4. When doping with F, F atoms are covalently bonded with edge-gN and edge-2gN to form edge-gN-F and edge-2gN-F, pyrrolic N active sites edge pyrrolic N-F were also formed. According to the FED results, all the active configurations with F doping are more prone to produce CO. With the DFT data, CO_2 reduction mechanism could be described by the CHO * pathway (Fig. 4d). In summary, the experiment and computational results in this study reveal the specific role of different heteroatom doping towards the selectivity and activity of CO_2 electroreduction. N-doping carbon provides active sites for CO_2RR. Meanwhile, the F-doping plays an important role in regulating the CH_4 selectivity of CO_2RR, with the decreasing of the F-doping level, the reduction is more favorable towards CO instead of CH_4. Additionally, Cl-doping also shows enhanced selectivity towards CH_4. This work offers great guidance for designing COF-based CO_2RR catalysts by heteroatom doping method.

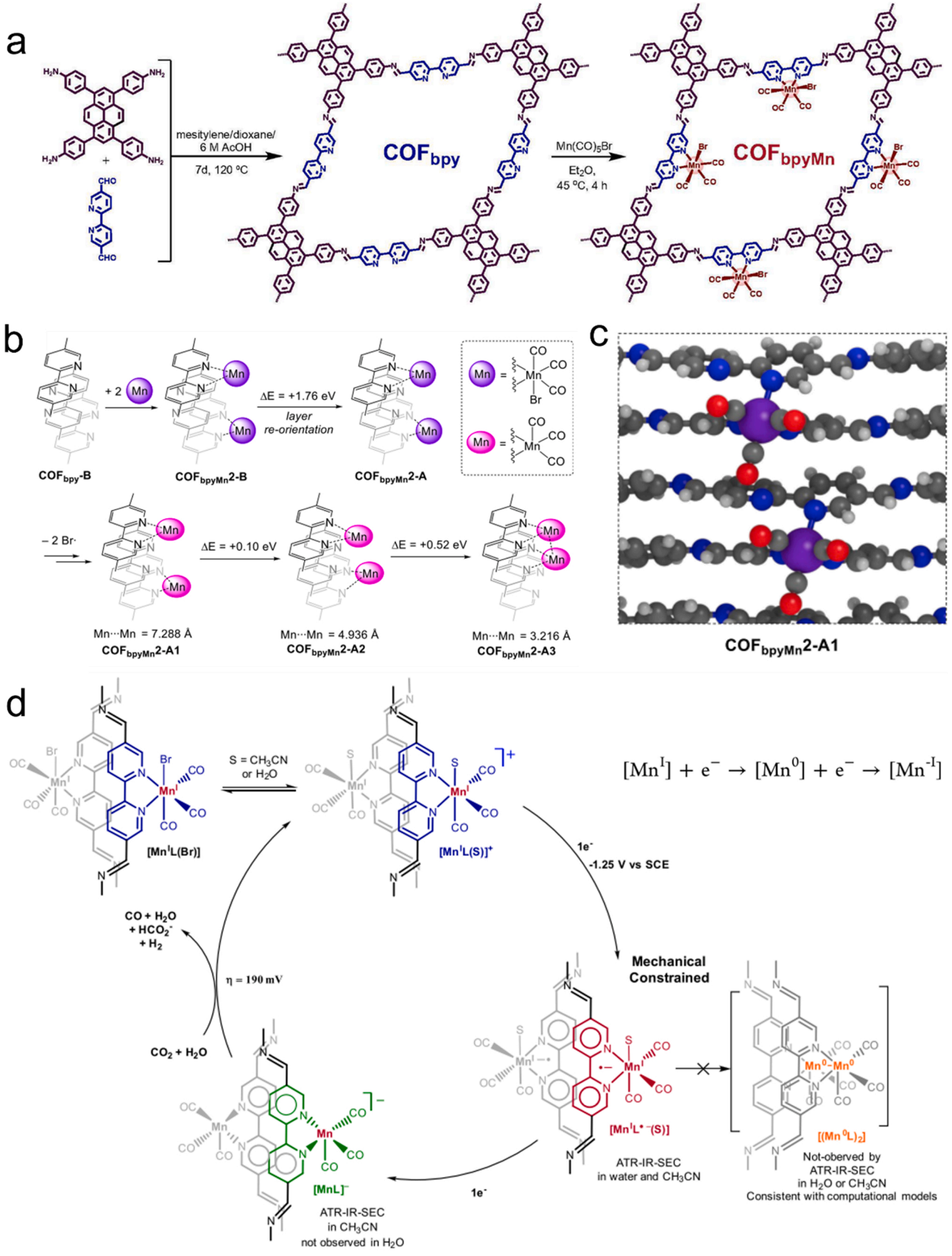

Fig. 3. a) Synthesis of COF_{bpy} and COF_{bpyMn} catalyst; b) DFT energies of the endergonic dimerization process of the COF; c) optimized structure for COF_{bpyMn}2-A1; d) Proposed mechanism for electrocatalytic CO_2 reduction in COF_{bpyMn} [38].

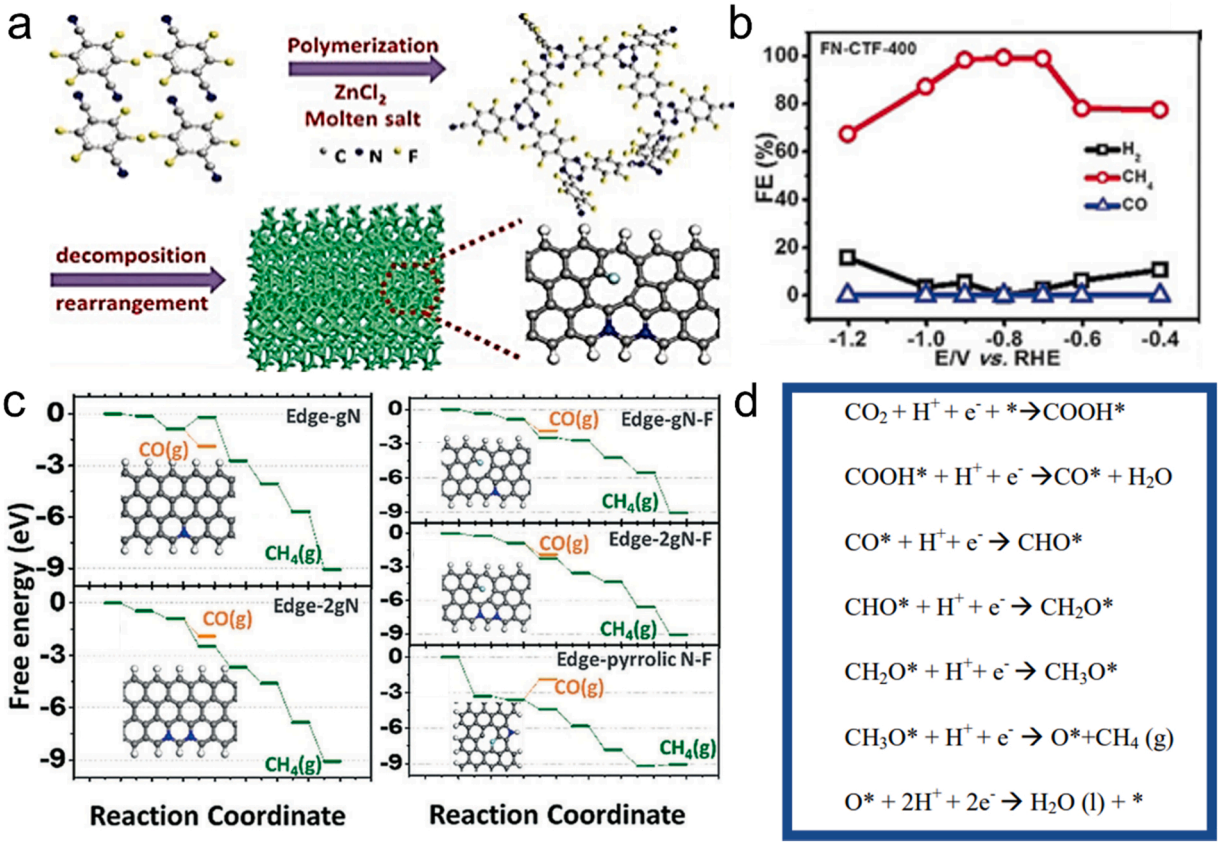

Fig. 4. a) Synthesis and the structure of FN-CTF-400; b) Faradaic efficiencies for CH_4, CO, and H_2 versus the potential on FN-CTF-400; c) Top views of the heteroatom doping structure and the DFT calculated reaction FED of the active sites for CO_2 electroreduction (C, H, N and F are present in grey, white, blue and cyan, respectively); d) CH_4 formation mechanism through the CHO * pathway [45].

The performance of the above-mentioned and selected COFs catalysts for electrochemical CO_2RR are all tabulated in Table 2.

4. Photocatalytic CO_2 reduction

Directly utilizing solar energy to convert CO_2 into valuable chemicals has been considered one of the most promising strategies to tackle global warming, climate changes, and energy supply sustainability [50]. Covalent organic frameworks have recently obtained the focus of the scientific community in regard to its potential for photocatalytic carbon dioxide reduction. This emerging class of materials has many inherent advantages for photocatalysis, including highly ordered and porous structure for mass transfer, ordered crystalline structure for reduced chance of charge recombination, excellent thermal and chemical stability for various reaction medium and conditions, rich heteroatoms (e.g. nitrogen atoms) in their skeletons, extensive conjugated π electric system both in plane and along the stacking directions for excellent light absorption and conductivity, and flexible reticular chemistry for modulating band gap or structure properties [11]. COFs serving as a class of photocatalytic reduction catalysts are capable of producing various chemicals such as carbon monoxide, formic acid, and methanol among others depending upon the COF catalysts and their associated energy levels [1]. COFs can either independently function as photocatalysts or serve as functional supporting platforms to host active species in CO_2RR. The extent of COF research is still only in its infancy stage. This section summarizes the current progress of COF photocatalysts for CO_2RR. The principle, methods of designing photocatalytic COFs, as well as many different structures and components have been concluded, aiming to enlighten the scientific community for future advancement in COF photocatalysts research.

4.1. Pristine COFs: Metal-free catalyst

Through recent research, COFs without the use of metalated active centers, have been used for the photocatalytic reduction of carbon dioxide. It is evident that the overall reduction potential and efficiency are much less than that of metallic supplemented COFs, but metal-free COFs offer advantages based on sustainability and scalability of future carbon dioxide reduction projects.

The 2D triazine-based covalent organic framework, built from cyanuric chloride and 3,4,9,10-Perylenetetracarboxylic diimide by Yadav et al. in 2016, is the first reported COF material for photocatalytic CO_2 reduction [51]. In this early research, the synthesized COF in the presence of enzyme and rhodium complex converted CO_2 to formic acid. When compared to the monomer counterpart catalyst, the COF catalyst obtained 3.4 times higher HCOOH formation in the same time period (881.3×10^6 nmol/g_{cat}/h for the COF vs. 261.85×10^6 nmol/g_{cat}/h for the monomer). It is concluded that the better performance is originated from the systematic arrangement of light harvesting units with spatial orientation and the columnar stacking structure of highly ordered π electron channel systems to promote charge transport. Following the path, Fu et.al. reported two azine-based COFs (ACOF-1 and N_3-COF) to reduce carbon dioxide to methanol as a primary product under visible light irradiation [52]. It is noteworthy that the catalysis is done in H_2O without any sacrificial agents like triethanolamine, a common sacrificial electron donor. But their activities are not very competitive. To further advance metal-free COF photocatalytic materials, a 2D donor-acceptor (D-A) COF (CT-COF) prepared by the Schiff base reaction of carbazole-triazine based D-A monomers, was developed where electron-rich carbazole moiety possesses excellent hole-transporting capability and triazine-based moieties of large electron affinity offers

Table 2
Summary of electrochemical CO_2RR performance with COF related materials.

Catalysts	Electrolyte	Conductivity	Product Efficiency	Ref.
COF-366-Co	0.5 M $KHCO_3$ solution	$\sim 10^{-8}$ S m^{-1}	FE_{CO} = 90%	[26]
COF-367-Co		N/A	FE_{CO} = 91% $TON_{EA} \approx$ 48,000	
COF-366-F-Co	0.5 M $KHCO_3$ solution	N/A	FE_{CO} = 87% J_{CO}= 65 mA mg^{-1}	[27]
COF-366-$(OMe)_2$-Co@CNT	0.5 M $KHCO_3$ solution	N/A	FE_{CO}= 93.6% at −0.68 V J_{CO}= 40 mA cm^{-2} at −1.05 V	[35]
TAPP(Co)-B18C6-COF	0.5 M $KHCO_3$ solution	7.2×10^{-8} S m^{-1}	FE_{CO}= 90.5% TOF= 1267 h^{-1}	[31]
TT-Por (Co)-COF	0.5 M $KHCO_3$ solution	1.38×10^{-8} S m^{-1}	FE_{CO}= 91.4% at −0.6 V J_{CO}= 7.28 mA cm^{-2} at −0.7 V	[33]
TTF-Por (Co)-COF	0.5 M $KHCO_3$ solution	1.32×10^{-7} S m	FE_{CO}= 95%	[32]
Co-TTCOF	0.5 M $KHCO_3$ solution	N/A	FE_{CO}= 99.7% at −0.8 V TOF= 1.28 s^{-1} at −0.7 V	[30]
CoPc-PDQ-COF	0.5 M $KHCO_3$ solution	3.68×10^{-3} S m^{-1}	FE_{CO}= 96% at −0.66 V TOF= 11,412 h^{-1}	[36]
CoPc-PI-COF-1	0.5 M $KHCO_3$ solution	3.7×10^{-3} S m^{-1}	FE_{CO}= 93% TOF= 2.2 S^{-1}	[37]
COFbpyMn	0.5 M $NaHCO_3$ solution	N/A	FE= 72% TOF 1100 h^{-1}	[38]
FeDhaTph-COF	MeCN with 0.5 M trifluoroethanol	N/A	FE_{CO}= 80% TOF 600 h^{-1}	[39]
Cu-Tph-COF-Dct	1 M KOH solution	N/A	FE_{CH4}= 80% Jco= −220 mA cm^{-2}	[40]
NiPor-CTF	0.5 M $KHCO_3$ solution	N/A	FE_{CO}= 97% at −0.9 V Jco= 52.9 mA cm^{-2}	[48]
Ni-CTF	$KHCO_3$ electrolyte	N/A	FE_{CO}= 90% at −0.8 V	[41]
COF-2,2′-bpy-Re	0.1 M tetrabutylammonium hexafluorophosphate acetonitrile	N/A	FE_{CO}= 81%	[49]
COF-Re_Co	0.5 M $KHCO_3$ solution	N/A	FE_{CO}= 18(2) %	[34]
FN-CTF-400	0.1 M $KHCO_3$ solution	N/A	FE_{CH4}= 99.3%	[45]
TTF-1	0.5 M $KHCO_3$ solution	3930 S m^{-1}	FE_{CO}= 82% at −0.68 V Jco= 3.2 mA cm^{-2} at −0.9 V	[44]
F-CTF-1–275	1 M KOH solution	N/A	FE_{CO}= 95.7% at −0.8 V Jco= −118 mA cm^{-2}	[46]
HATCTF@MWCNT-OH	0.1 M $KHCO_3$ solution	N/A	FE_{CO}= 81% Jco= −0.48 mA cm^{-2}	[47]
MWCNT-Por-COF-Co	0.5 M $KHCO_3$ solution	N/A	FE_{CO}= 99.3% at −0.6 V Jco= 18.77 mA cm^{-2} at −1 V	[28]
MWCNT-PorCOF-Cu	1 M KOH solution	N/A	FE_{CH4}= 71.2% at −1 V	[28]

high electron drift mobility [53]. The CT-COF photocatalyst with the rationally incorporated D-A heterojunction structure provides the advantage of narrow band gap and promoted exciton splitting and charge transport, which was able to reduce CO_2 to CO as the main carbonaceous product in the presence of gaseous H_2O without any co-catalysts (CO evolution rate 102.7 μmol g^{-1} h^{-1}). It was also observed that the approximate stoichiometric O_2 evolution happened simultaneously. Another β-ketoenamine-based 2D COF, termed TpBb-COF, performed photocatalytic reduction of CO_2 to CO in gas-solid system without using other additives [54]. It is interesting that TpBb-COF exhibited better performance in diluted CO_2 atmosphere (30.0%) than a pure one at 80 ° C, 89.9 μmol g^{-1} h^{-1} versus 52.8 mmol μmol g^{-1} h^{-1}. The possible reason could be the production rate of CO is proportionated differently at different CO_2 concentration. In a recent work, Peng et. al studied the influence of different functional groups in the same primary COF for photocatalytic CO2 reduction [55]. A group of TpBD samples with different functional groups, termed TpBD-X (X = -H_2, -$(CH_3)_2$, -$(OCH_3)_2$ and –$(NO_2)_2$), were prepared through the amine-aldehyde condensation of 1,3,5-triformylphloroglucinol and the corresponding diamine, followed by an irreversible enol-keto tautomerism to form a β-ketoenamine bond (Fig. 5). As a result, the functional groups of different electron-donating capability can regulate the electronegativity of TpBD-X, and thus allow the tuning of their light absorption and photogenerated charge separation ability. The corresponding photocatalytic reduction of CO_2 to HCOOH for TpBD-H_2, TpBD-$(CH_3)_2$, TpBD-$(OCH_3)_2$, and TpBD-$(NO_2)_2$ are 45.7, 86.3, 108.3, and 22.2 μmol g_{cat}^{-1} h^{-1}, respectively. Although the photocatalytic activity is lower than most of the reported metal-based COF photocatalytic systems, this work demonstrates a promising approach of fine-tuning catalyst properties via functional group variation.

4.2. Metalated COFs

Metalated or hybrid COF materials offer increased effectiveness of photocatalytic effects due to their increased ability of charge transfer. Therefore, metal complexes (e.g. Re, Ru, Mn complexes) or other catalysts (e.g. TiO_2, metal single sites) are often incorporated into COFs photosynthesis [11]. COFs in the composites catalysts act as either photosensitizers or functional support. In 2018, Huang's group pioneeringly coupled tricarbonylchloro(bipyridyl) Re complex (Re(bpy)$(CO)_3Cl$) as CO_2 reduction molecular catalyst (denoted Re-COF) to a photoactive 2D triazine COF which is acting as a photosensitizer [56]. The synthesis procedure and catalytic mechanism is shown in Fig. 6. Under visible light illumination, the Re-COF catalyst efficiently reduced CO_2 to CO with high electivity (98%) and better activity than its homogeneous Re counterpart. The same group later incorporated Mn complex ($Mn(CO)_3$(BPy)Br (BPy=2,2′-bipyridyl)) to the same COF photosensitizer. Mn complex was found to be unstable and led to low photocatalytic activity and short duration due to the elimination of CO ligand in Mn complex upon light illumination. Despite the poor performance, $Mn(CO)_3$(BPy)Br in COFs still showed much longer duration and higher TON than its homogeneous version, confirming the role of COFs as a great platform [57]. Bipyridine-based covalent organic

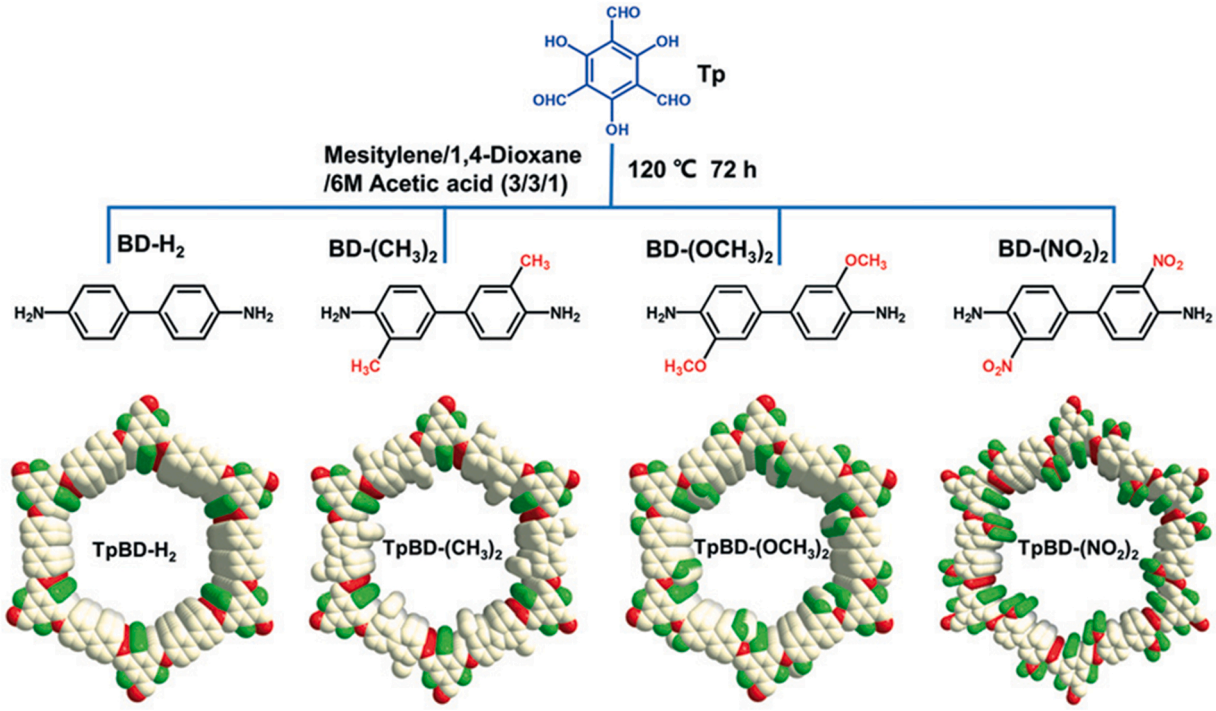

Fig. 5. Synthesize and the structure of TpBD-X [X = $-H_2$, $-(CH_3)_2$, $-(OCH_3)_2$, and $-(NO_2)_2$] [55].

frameworks were also applied to embed photoactive rhenium complex ($Re(CO)_5Cl$) [58]. The bipyridine groups in the COF channels offered uniform coordination sites for the chelation with Re complex, generating isolated and molecularly defined catalytic sites. The COF supported molecular catalyst showed 2 times higher CO production than that of a Re reference compound. Bipyridine COFs with increased conjugation length in the framework were also used to host $Re(CO)_5Cl$ [59]. This Re-COF was able to achieve 81% selectivity of CO production. When a photosensitizer was introduced, the selectivity increased to 86%. Further loading platinum to the catalyst, syngas (H_2 and CO) was the product and the composition ratio can be adjusted by the amount of platinum. This work also demonstrated that the crystallinity of the COF is beneficial to its photocatalytic performance in CO_2 reduction in comparison with the control study of an amorphous analog of the COF.

Like electrocatalysis, cobalt and zinc are highly effective metallic centers but, in this case, providing photocatalytic activity. Studies on Co-, Ni-, Zn-based COFs catalyst have been on the rise due to their promising performance. The two main reduction products disregarding reaction selectivity for metallic active site COFs are carbon monoxide and formic acid. Lan et al. incorporated different metal active species (M=Co(II) /Ni(II) /Zn(II)) into 2D anthraquinone-contained COF (termed COF-M), and further detailed the selectivity effects of the metal sites [50]. Two photocatalytic CO_2 reduction pathway were proposed (Fig. 7), where the product is dependent on the pathway the catalyst tends to proceed. On one hand, the electron donor ability tends to create an electron-rich coordination environment that can weaken and break the C-O bond which tends to form CO (Pathway 1). On the other hand, electron withdrawal ability tends to form an electron deficiency coordination environment that can enhance the C-O bonding force leading to the formation of HCOOH (Pathway 2). The proposed mechanisms were further confirmed by the experiment results where the good π-donor ability of Co(II) allows for selective carbon monoxide production whereas the poor π-donor Zn(II) allows for selective formic acid production. For COF-Ni(II), a nearly equal amount of CO and HCOOH was produced. It was the quinone oxygen atom in the COF that is crucial for immobilizing the metal ions, in comparison with a similarly structured COF lacking suitable oxygen coordination sites. Single Ni sites anchored on 2,2′-bipyridine-based COF (Ni-TpBpy) as a synergistic catalyst demonstrated selective photoreduction of CO_2 to CO under the presence of $Ru(bpy)]_3Cl$ photosensitizer and TEOA electron donor. DFT calculation revealed single Ni sites has preferred affinity with CO_2 over H^+, and thus inhibiting H_2 formation. Ni sites is where CO_2 molecules are coordinated, activated, and reduced, and the TpBpy COF host contributes to the activity and selectivity as well [60]. Yang et. al. studied the effect of linkage microenvironment on the catalytic performance, by comparing nickel modified N-acylhydrazone-linked COF containing triphenylamine donor and triphenyl-1,3,5-triazine acceptor (H-COF-Ni) with the imine-linked counterpart (I-COF-Ni) [61]. H-COF-Ni effectively produced 5694 μmol g^{-1} of CO with 96% selectivity over H_2 evolution in 2 h, much greater performance than that of I-COF-Ni. Instead of the separation and transfer process of the photogenerated charge carriers as the main reason, the more favorable activation of CO_2 on Ni sites in N-acylhydrazone linkage contributed to higher CO_2 to CO conversion activity. H-COF-Ni has the Ni-C bond length of 3.074 Å (shorter than the 3.277 Å of I-COF-Ni) and the CO_2 adsorption energy on Ni of −0.58 eV (more negative than the −0.28 eV of I-COF-Ni), confirming the profound influence of local microenvironments.

In terms of Co active sites, a donor-acceptor type Co-PI-COF, composed of isoindigo and cobalt metallated porphyrin subunits, was developed to catalytically reduce CO_2 to formate. The efficient charge carrier separation, low band gap (0.72 eV), and strong CO_2 adsorption at coordinatively unsaturated cobalt centers is the key to the reported performance (~50 μmol g^{-1} h^{-1}) [64]. It was also reported that a synthesized TFPG-DAAQ COF was able to reduce CO_2 into HCOOH when mixing with a cobalt co-catalyst and the TEOA sacrificial electron source [65]. Catalysts' electronic structure has tremendous impact on catalysis. To understand the electron spin regulation over performance, Gong et. al. manipulated the cobalt spin state over COF-367-Co by simply changing the oxidation state of Co center in the porphyrin. It was concluded that Co^{II} and Co^{III} are embedded in COF-367 with S = 1/2 and 0 spin ground states, respectively (Fig. 8a) [62]. COF-367-Co^{III} showed favorable activity and significantly enhanced selectivity to HCOOH, accordingly much reduced activity and selectivity to CO and CH_4, starkly different from photocatalytic behavior of COF-367-Co^{II}. This

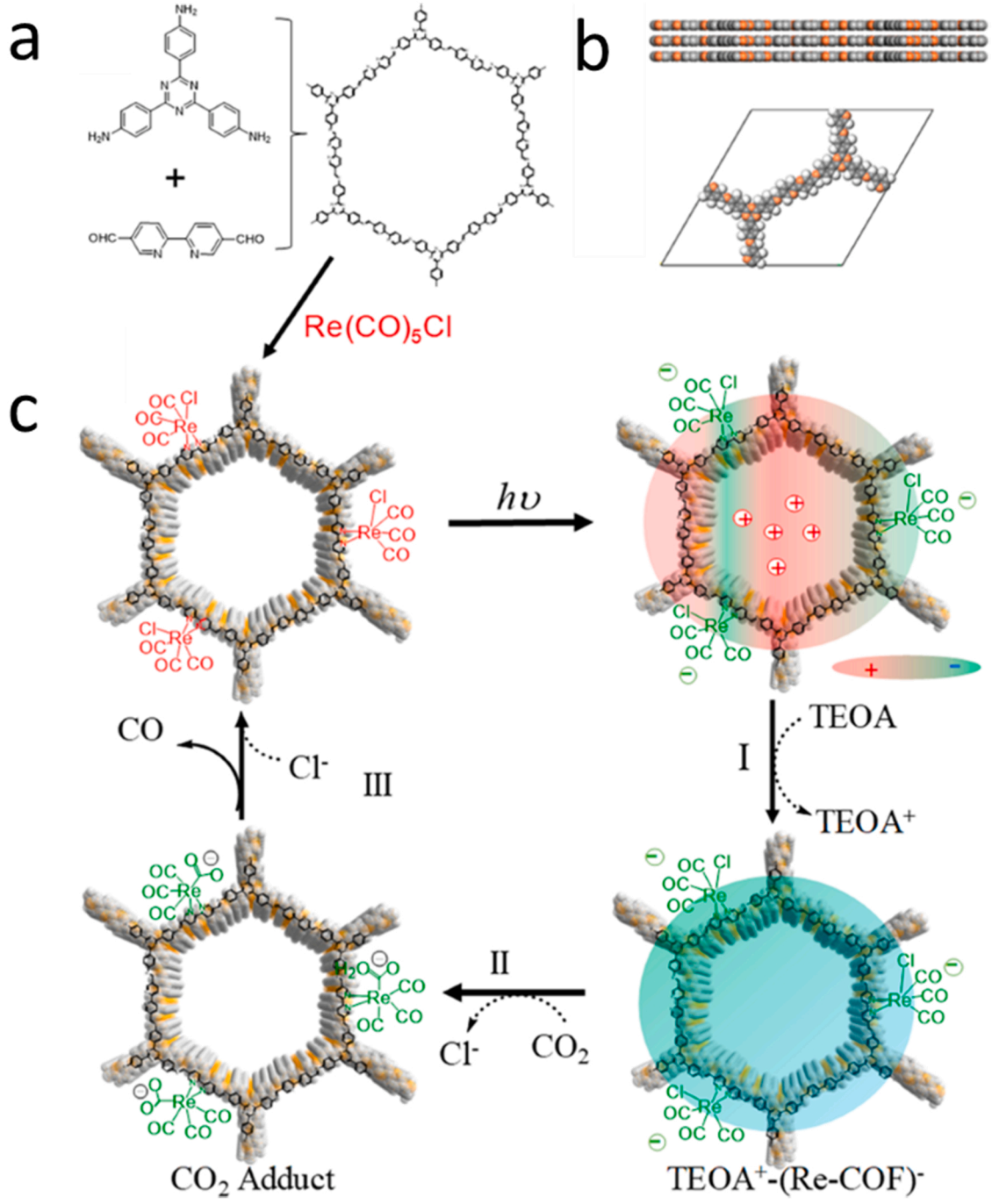

Fig. 6. a) Synthesize of COF and Re-COF; b) Side view and unit cell of AA Stacking COF; c) Proposed catalytic mechanism for CO_2 reduction [56].

work represents a great process on the fundamental understanding of spin state manipulation in catalyst design for CO_2 reduction. A series of crystalline 2D rigid porphyrin-tetrathiafulvalene COFs (TTCOF-M, M = 2H, Zn, Ni, Cu) were synthesized for selective photoreduction of CO_2 with H_2O as an electron donor, namely, coupled CO_2 reduction and H_2O oxidation half-reactions (Fig. 8b) [63]. Among them, TTCOF-Zn showed the highest CO evolution of 12.33 μmol under visible light illumination after 60 h with ~100% selectivity and remarkable durability under the experimental conditions. Noteworthy, most reported COFs in the photocatalysis are 2D based, possibly owing to the large surface and abundant active sites on the surfaces. Top-down strategies that exfoliate bulk counterparts to form 2D COFs suffers from low yields, uncontrollable thickness, and possible mechanical damage due to the strong interlayer π−π interactions in the bulk 2D COFs. Liu et. al. reported a scalable general bottom-up approach to prepare a series of ultrathin (<2.1 nm) imine-based 2D COF Nanosheets (NSs) (including COF-366 NSs, COF-367 NSs, COF-367-Co NSs, TAPB-PDA COF NSs) in large scale (>100 mg) and high yield (>55%) [66]. It is an imine-exchange synthesis strategy under solvothermal conditions with large excess amounts of 2,4,6-trimethylbenzaldehyde into the reaction system. COF-367-Co NSs showed excellent performance for CO_2-to-CO conversion (10,162 μmol g^{-1} h^{-1}, ca. 78% selectivity) in aqueous media under visible-light irradiation. Both the process and nanosheets images are shown in Fig. 9.

4.3. Hybrid COFs

In addition to active metal sites, some recent work started to use COFs to host nanoparticles and carbon dots. Considering noble metal

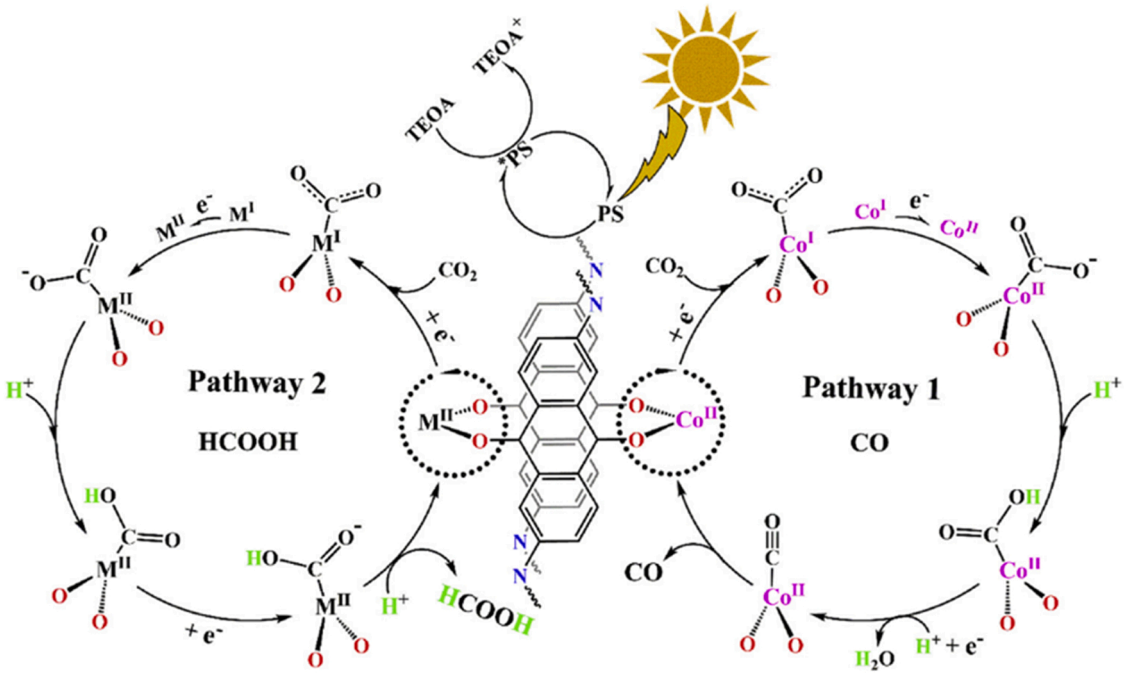

Fig. 7. Proposed mechanisms for photocatalytic reduction of CO_2 with DQTP COF-M (M=Zn, Co, Ni) catalysts [50].

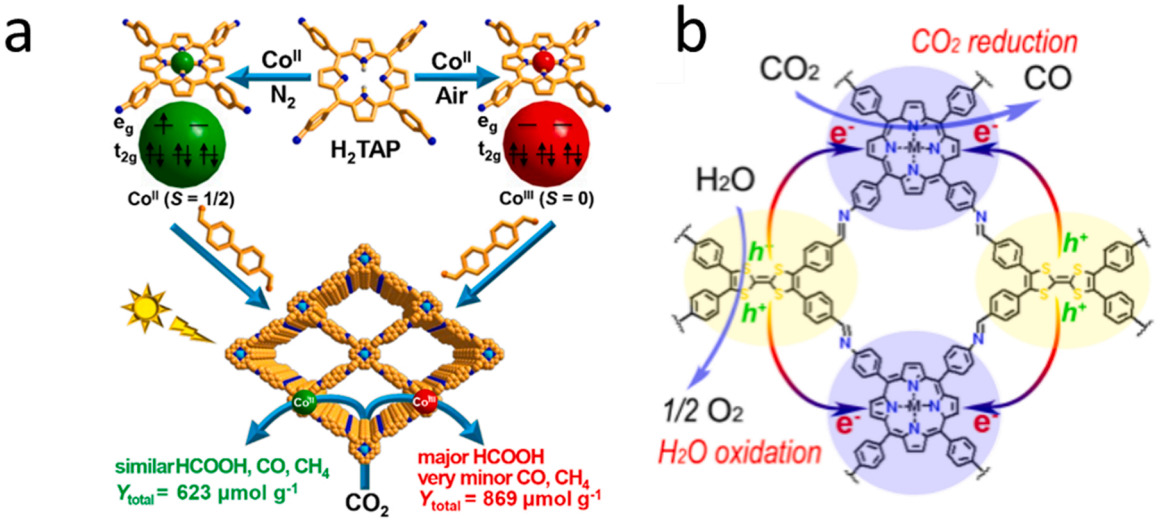

Fig. 8. a) COF-367-Co with different spin states of Cobalt ions toward photocatalytic CO_2 reduction;[62] b) Proposed mechanism of TTCOF-M CO_2RR with H_2O oxidation [63].

nanoparticles (NPs) are highly effective on the suppression of the electron-hole recombination and COFs with distinctive microenvironments serve as excellent functional supports, Zhu and coworkers loaded different amount of Ru nanoparticles (NPs) to ketoamine based COF (TpPa-1) and bipyridine-linked COF (TpBpy) via post synthesis, respectively, named Ru/TpPa-1 and Ru@TpBpy [11,67]. 3.0 wt% Ru/TpPa-1 had maximum HCOOH production rate of 108.8 μmol g_{cat}^{-1} h^{-1}, and 0.7 wt% Ru@TpBpy with HCOOH production rate of 172 μmol g_{cat}^{-1} h^{-1}, indicating the critical role of the properties of COF support. Semiconducting materials has also been incorporated to COFs for CO_2 reduction [68,69]. Post-synthesized NPs on COFs mostly are secured via physical adsorption, which could be unstable and affect catalyst durability, and thus it is desired to build a chemical link between the NPs and COF host. By conducting COF synthesis in the presence of semiconducting materials (TiO_2, Bi_2WO_6, and α-Fe_2O_3), shown in Fig. 10, Lan et al. developed a stable covalently bonded organic-inorganic Z-scheme system between semiconductor and COFs for CO_2 reduction with H_2O as electron donor, absent of any additional photosensitizers, sacrificial agents, and co-catalysts. The covalent bond linked COF-318-TiO_2 Z-scheme heterojunction showed the highest CO production rate of 69.67 μmol/g/h, much higher than the physical mixture composites [69]. It is concluded that covalent coupling between organic framework and semiconductor effectively facilitates the charge transfer in the catalysis. Another Z-scheme hybrid structure between TiO_2 and metalloporphyrin block-based COF reported a CO production rate of 50.5 μmol g^{-1} h^{-1}, supporting the same conclusion [68].

Zhong et. al. reported a pioneering work on metalloporphyrin-based carbon dots hosted in the cavities of COFs as the active sites (M-PCD@TD-COF, M = Ni, Co, and Fe)) for visible-light-driven CO_2 reduction [70]. With COFs providing beneficial microenvironment for

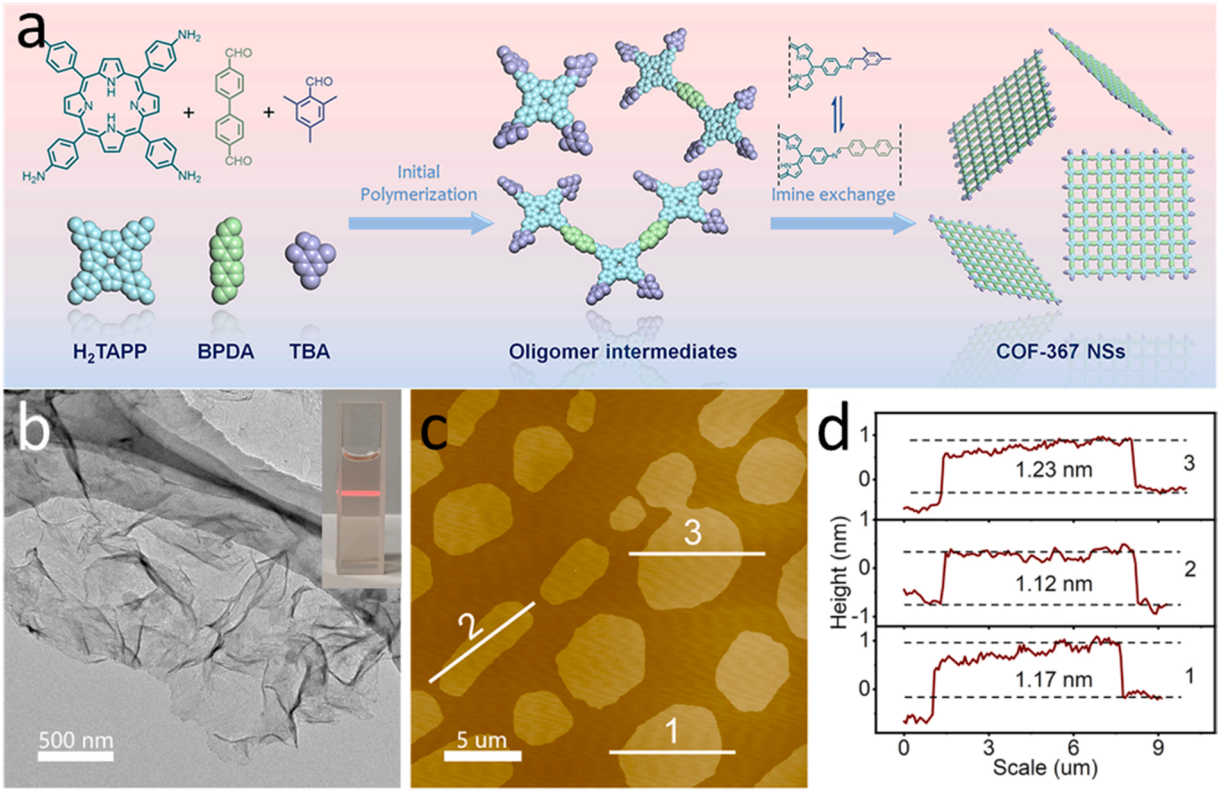

Fig. 9. a) Schematic of Synthesis of the COF-367 NSs; b) TEM (transmission electron microscopy) image of COF-367 NSs (inset shows the photo of the Tyndall effect of COF-367 NSs dispersion in EtOH); c) AFM image and d) the height profiles along the marked white line of COF-367 NSs [66].

CO_2 adsorption and the activation on metalloporphyrin active sites, the selectivity of CO_2-to-CO conversion over H_2 generation reached 98%. The composite catalysts were also highly stable, showing no inappreciable loss of catalytic activity and selectivity in five repeated runs. It represents a promising category of COF materials for development. The performance of the above-mentioned and recent COFs catalysts for photocatalytic CO_2RR are summarized in Table 3.

5. Coupled driving forces for CO_2RR

In the previous sections, electrochemical and photocatalytic CO_2 reduction is solely driven by electric energy and solar energy, respectively. Another rather promising insight into the future of COF research is to couple different driving forces (e.g., photocoupled electrocatalytic reduction of carbon dioxide). Photon energy will interfere with the electronic properties of light sensitive electrocatalysts, possibly changing the electrochemical catalytic process and activity. Catalysts for such systems need to possess high stability under photo irradiation and electric energy, effective catalytic active sites for CO_2 reduction, and great light absorption and photo-electron conversion capabilities. Lan et.al. reported a series of highly stable dioxin-linked metallophthalocyanine 2D-COFs (MPc-TFPN- COF, M = Ni, Co, Zn) designed for such system [15]. The study found that an external light-field can enhance the electron transfer to the adsorbed CO_2 in phthalocyanine COFs, and thus benefit the reduction of CO_2. Quantitative comparison showed that coupling the driving forces of light and electricity improved the FE_{CO} and current density (j_{CO}) at all applied potential range (−0.6 to −1.2 V vs. RHE). Compared to the dark environment, NiPc-TFPN COF had j_{CO} increased from 14.1 to 17.5 mA cm^{-2} at −0.9 V; FE_{CO} reached up to ~100% at −0.8 to −0.9 V; the overpotential for the maximum FE_{CO} positively shifted about 100 mV. The encouraging results indicated this is a promising route into maximizing efficiency and sustainability in the future of COF based catalysts.

Moreover, a recent work reported COFs for photocatalyst-enzyme coupled system of CO_2 reduction, representing an alternative route to boost performance [72]. Specifically, mesoporous olefin-linked COF (NKCOF-113) was used as a carrier to co-immobilize formate dehydrogenase (FDH) and Rh-based electron mediator, as shown in Fig. 11 This COF catalyst enabled highly selective photocatalytic conversion of CO_2 to formic acid. This work that anchored both metal complex and biologic enzyme into COFs, realized the effective cascade of chemical and biological catalysis, further demonstrated the enormous potential of COF materials for CO_2 reduction.

6. Summary & outlooks

This review summarizes the progress of COF-based catalysts for electrochemical and photocatalytic CO_2RR. These COF-based catalysts show enhanced performance compared with molecular catalysts in activity and selectivity. The advantages of COFs in CO_2RR can be ascribed to their unique structure and properties. Their porous structure facilitates the accessibility of CO_2 during the reaction allowing more effective exposure of active sites. The design flexibility of COFs allowed the convenient modification of COF structure. For example, there are numerous choices of ligands, and ligands can be easily modified by introducing functional groups and heterogeneous doping, which helps catalysts to achieve enhanced absorption of CO_2, regulated selectivity, thermal and chemical stability, as well as enhanced conductivity. On the other hand, a wide range of metal sites can be incorporated into predetermined COF structures. The control on the loading, local structure, and microenvironment of metal sites offers unprecedented opportunities to further advance COFs catalyst design. Other materials (semiconductors, active nanoparticles, or enzymes) can also be bonded to COFs, offering more opportunities for catalysis. Overall, COF-based CO_2RR catalysts are promising for carbon neutralization.

Despite the advantages of COF catalysts, the main barrier that limits

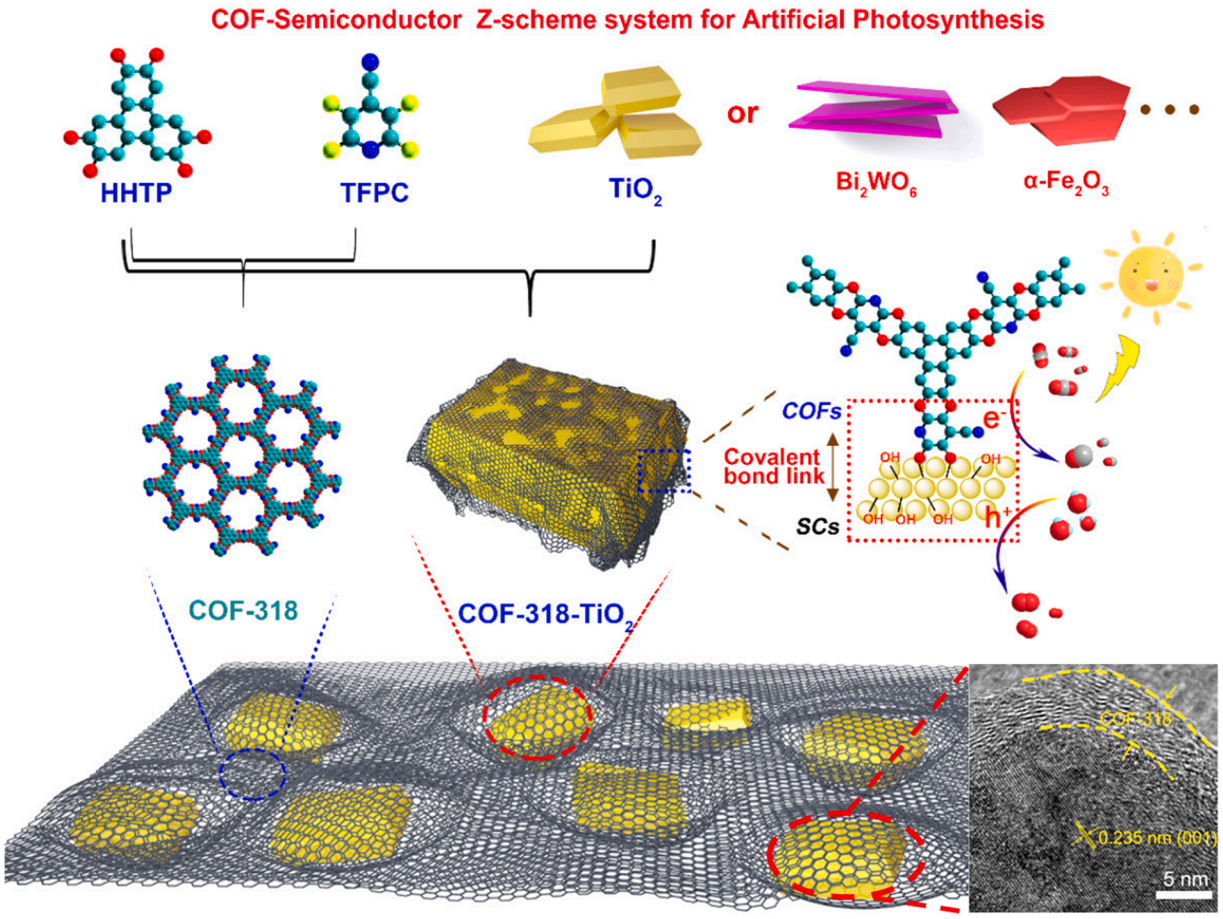

Fig. 10. Schematic of the synthesize of COF-318-SCs via the condensation of COF-318 and semiconductor and proposed mechanism of COF-318-SCs CO_2RR [69].

Table 3
Summary of photocatalytic CO_2RR performance with COF related materials.

Catalysts	Light Source	Wavelength (nm)	bandgap (eV)	Yield (μmol/ (g_{cat}*h)	Optimal Selectivity	Ref.
CTF	Xe Lamp	420	2.05	881.3 × 10^3 HCOOH	N/A	[51]
N_3-COF	Xe Lamp	800 ≥ λ ≥ 420	2.6	0.57 CH_3OH	N/A	[52]
CT-COF	Visible Light	≥ 420	2.04	102.7 CO	FE_{CO}= 98%	[53]
TpBb-COF	Visible Light	380	1.72	89.9 CO	FE_{CO}= 99%	[54]
TpBD-$(CH_3)_2$	Visible Light	800 ≥ λ ≥ 420	2.17	108.3 HCOOH	N/A	[55]
Re-COF	Xe Lamp	420	N/A	N/A	FE_{CO}= 98%	[56]
Mn-TTA-COF	Xe Lamp	420	N/A	1700	N/A	[57]
Re-TpBpy COF	Xe Lamp	> 390	N/A	N/A	N/A	[58]
Re-Bpysp2 c-COF	Xe Lamp	> 420	N/A	1400 CO	$FE_{CO/H2}$= 86%	[59]
H-COF-Ni	Visible Light	> 420	2.48	2847 CO	$FE_{CO/H2}$= 96%	[61]
Co-PI-COF	Xe Lamp	800 ≥ λ ≥ 420	0.56	50 HCOOH	N/A	[64]
TFPG-DAAQ COF	Blue LED Light	445	N/A	N/A	N/A	[65]
COF-367-Co(II)	Xe Lamp	380	1.03	48.6 HCOOH	FE= 96.8%	[62]
COF-367-Co(III)	Xe Lamp	380	1.10	93.0 HCOOH	FE= 97.1%	[62]
TTCOF-Zn	Visible Light	800 ≥ λ ≥ 420	1.49	N/A	FE_{CO}~100%	[63]
COF-367-Co NSs	Xe Lamp	> 420	N/A	10162 CO	FE= 78%	[66]
0.7 wt% Ru@TpBpy	Xe Lamp	800 ≥ λ ≥ 420	N/A	172 HCOOH	N/A	[67]
Ru/TpPa-1	Xe Lamp, light filter	350	N/A	108.8 HCOOH	N/A	[11]
TpPa-1	Xe Lamp, light filter	350	N/A	32.4 HCOOH	N/A	[11]
1.5% TiO_2-INA@CuP-Ph COF	Xe Lamp	N/A	2.60	50.5 CO	N/A	[68]
Ni-TpBpy	Visible Light	N/A	N/A	811.4 CO	FE_{CO}= 96%	[60]
Ni-PCD@TD-COF	Xe Lamp	> 420 nm	1.69	478 CO	FE_{CO}= 98%	[70]
COF-318-TiO_2	Simulated Sunlight Irradiation	800 ≥ λ ≥ 380	N/A	69.67 CO	N/A	[69]
CTF-BP	Xe Lamp	> 420 nm	N/A	7.81 CH_4 4.60 CO	N/A	[71]

their practical applications is synthesis. COFs usually require harsh synthesis conditions, including high cost, tedious procedures, low yields, long duration, post purification, and involvement of organic solvents. Cost-effective, facile, and scalable COF synthesis is an urgent field requiring effort from the scientific community.

In addition, it also calls attention to inhibiting competitive proton

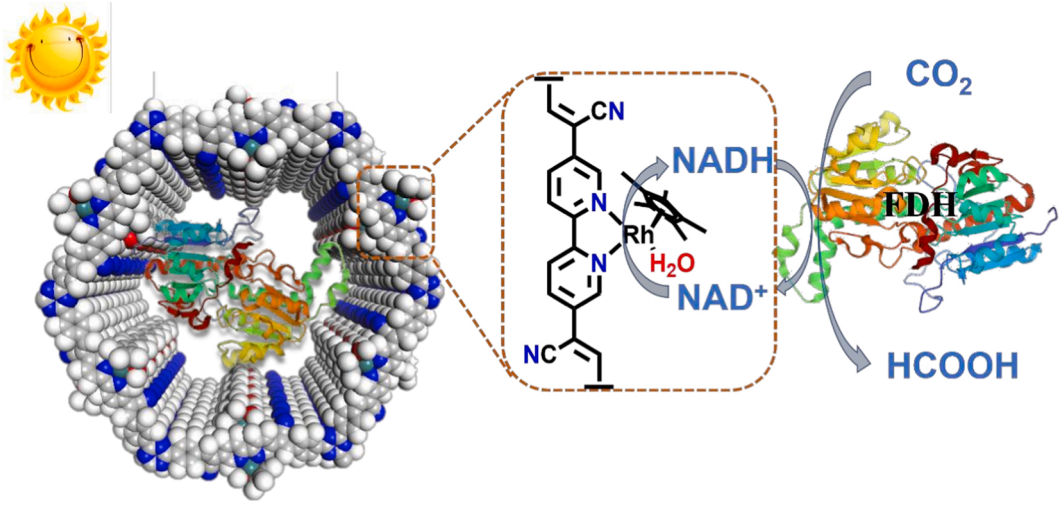

Fig. 11. Schematic of the proposed photo-enzymatic system converts CO_2 to formic acid under visible light [72].

reduction as well as improving selectivity for carbonaceous products. Moreover, balancing the hydrophobicity and hydrophilicity of the COF remains a challenge. The hydrophobicity can inhibit the competing HER reaction while hindering the access of electrolytes. How to find a balance of this parameter still requires more effort. Finally, the catalytic mechanism and catalytic activity decay have not been fully understood or explained. More research should be undertaken to understand the fundamental aspects of COF electrocatalysts.

There are some unexplored areas involving COFs for CO_2RR. Since CO_2 is a highly stable substance, it requires high energy to break the bonds. Coupling reaction driving forces together could significantly boost catalytic performance in a complementary way. Some examples include photo-electrochemical, photo-thermal, electrochemical-thermal, and photo-enzymic energy sources. Additionally, some recent reports on carbon-based electrocatalysts derived from COFs for ORR and other applications demonstrated promising performance. To the best of our knowledge, no such catalyst for CO_2RR has been reported. This could be a possible new direction to explore. Overall, with continuous and growing research effort, COFs and their derivatives will significantly advance fundamental knowledge on chemistry and materials design as well as play a critical role in CO_2RR catalysis for carbon neutralization.

CRediT authorship contribution statement

Zizhou He: Writing – original draft. **Joshua Goulas:** Writing – original draft. **Evana Parker:** Editing and suggestions. **Yingqiang Sun:** Editing and suggestions. **Xiao-dong Zhou:** Discussion and editing. **Ling Fei:** Conceptualization, Supervision.

Declaration of Competing Interest

The authors declare of no conflict of interests.

Acknowledgements

LF and XDZ thank the support from NSF, USA under NSF-2119688.

References

[1] H. Wang, H. Wang, Z. Wang, L. Tang, G. Zeng, P. Xu, M. Chen, T. Xiong, C. Zhou, X. Li, D. Huang, Y. Zhu, Z. Wang, J. Tang, Covalent organic framework photocatalysts: Structures and applications, Chem. Soc. Rev. 49 (2020) 4135–4165.
[2] C. Singh, S. Mukhopadhyay, I. Hod, Metal-organic framework derived nanomaterials for electrocatalysis: Recent developments for CO_2 and N_2 reduction, Nano Converg. 8 (2021) 1.
[3] S.E.M. Elhenawy, M. Khraisheh, F. AlMomani, G. Walker, Metal-organic frameworks as a platform for CO_2 capture and chemical processes: Adsorption, membrane separation, catalytic-conversion, and electrochemical reduction of CO_2, Catalysts 10 (2020) 1293.
[4] X. Xuan, S. Chen, S. Zhao, J.Y. Yoon, G. Boczkaj, X. Sun, Carbon nanomaterials from metal-organic frameworks: A new material horizon for CO_2 reduction, Front. Chem. 8 (2020), 573797.
[5] C. Pettinari, A. Tombesi, Metal–organic frameworks for chemical conversion of carbon dioxide, MRS Energy Sustain. 7 (2020).
[6] C.A. Trickett, A. Helal, B.A. Al-Maythalony, Z.H. Yamani, K.E. Cordova, O. M. Yaghi, The chemistry of metal–organic frameworks for CO_2 capture, regeneration and conversion, Nat. Rev. Mater. 2 (2017) 17045.
[7] H. Zhang, M. Zhu, O.G. Schmidt, S. Chen, K. Zhang, Covalent organic frameworks for efficient energy electrocatalysis: Rational design and progress, Adv. Energy Sustain. Res 2 (2021), 2000090.
[8] K. Geng, T. He, R. Liu, S. Dalapati, K.T. Tan, Z. Li, S. Tao, Y. Gong, Q. Jiang, D. Jiang, Covalent organic frameworks: Design, synthesis, and functions, Chem. Rev. 120 (2020) 8814–8933.
[9] X. Zhao, P. Pachfule, A. Thomas, Covalent Organic Frameworks (COFs) for electrochemical applications, Chem. Soc. Rev. 50 (2021) 6871–6913.
[10] J. Ozdemir, I. Mosleh, M. Abolhassani, L.F. Greenlee, R.R. Beitle, M.H. Beyzavi, Covalent organic frameworks for the capture, fixation, or reduction of CO_2, Front. Energy Res. 7 (2019) 77.
[11] K. Guo, X. Zhu, L. Peng, Y. Fu, R. Ma, X. Lu, F. Zhang, W. Zhu, M. Fan, Boosting photocatalytic CO_2 reduction over a covalent organic framework decorated with ruthenium nanoparticles, Chem. Eng. J. 405 (2021), 127011.
[12] S. Tao, D. Jiang, Covalent organic frameworks for energy conversions: Current status, challenges, and perspectives, CCS Chem. 3 (2021) 2003–2024.
[13] X. Zhao, P. Pachfule, S. Li, T. Langenhahn, M. Ye, C. Schlesiger, S. Praetz, J. Schmidt, A. Thomas, Macro/Microporous covalent organic frameworks for efficient electrocatalysis, J. Am. Chem. Soc. 141 (2019) 6623–6630.
[14] M. Martínez-Fernández, R. Gavara, S. Royuela, L. Fernández-Ecija, J.I. Martínez, F. Zamora, J.L. Segura, Following the light: 3D-printed COF@poly(2-hydroxyethyl methacrylate) dual emissive ccomposite with response to polarity and acidity, J. Mater. Chem. A (2022).
[15] M. Lu, M. Zhang, C.G. Liu, J. Liu, L.J. Shang, M. Wang, J.N. Chang, S.L. Li, Y. Q. Lan, Stable dioxin-linked metallophthalocyanine Covalent Organic Frameworks (COFs) as photo-coupled electrocatalysts for CO_2 reduction, Angew. Chem. Int. Ed. 60 (2021) 4864–4871.
[16] Y. Chen, W. Li, X.-H. Wang, R.-Z. Gao, A.-N. Tang, D.-M. Kong, Green synthesis of covalent organic frameworks based on reaction media, Mater. Chem. Front. 5 (2021) 1253–1267.
[17] M.G. Kibria, J.P. Edwards, C.M. Gabardo, C.T. Dinh, A. Seifitokaldani, D. Sinton, E. H. Sargent, Electrochemical CO_2 reduction into chemical feedstocks: From mechanistic electrocatalysis models to system design, Adv. Mater. 31 (2019), e1807166.
[18] C. Costentin, M. Robert, J.-M. Savéant, Catalysis of the electrochemical reduction of carbon dioxide, Chem. Soc. Rev. 42 (2013) 2423–2436.
[19] M.B. Ross, P. De Luna, Y. Li, C.-T. Dinh, D. Kim, P. Yang, E.H. Sargent, Designing materials for electrochemical carbon dioxide recycling, Nat. Catal. 2 (2019) 648–658.
[20] Y.Y. Birdja, E. Pérez-Gallent, M.C. Figueiredo, A.J. Göttle, F. Calle-Vallejo, M.T. M. Koper, Advances and challenges in understanding the electrocatalytic conversion of carbon dioxide to fuels, Nat. Energy 4 (2019) 732–745.
[21] J. Qiao, Y. Liu, F. Hong, J. Zhang, A review of catalysts for the electroreduction of carbon dioxide to produce low-carbon fuels, Chem. Soc. Rev. 43 (2014) 631–675.

[22] X. Wang, M. Fan, Y. Guan, Y. Liu, M. Liu, T.N.V. Karsili, J. Yi, X.-D. Zhou, J. Zhang, MOF-based electrocatalysts for high-efficiency CO_2 conversion: Structure, performance, and perspectives, J. Mater. Chem. A 9 (2021) 22710–22728.
[23] K. Elouarzaki, V. Kannan, V. Jose, H.S. Sabharwal, J.M. Lee, Recent trends, benchmarking, and challenges of electrochemical reduction of CO_2 by molecular catalysts, Adv. Energy Mater. 9 (2019), 1900090.
[24] C.-Y. Lin, D. Zhang, Z. Zhao, Z. Xia, Covalent organic framework electrocatalysts for clean energy conversion, Adv. Mater. 30 (2018), 1703646.
[25] M. Usman, M. Humayun, M.D. Garba, L. Ullah, Z. Zeb, A. Helal, M.H. Suliman, B. Y. Alfaifi, N. Iqbal, M. Abdinejad, A.A. Tahir, H. Ullah, Electrochemical reduction of CO_2: A review of cobalt based catalysts for carbon dioxide conversion to fuels, Nanomater. (Basel) 11 (2021).
[26] S. Lin, C.S. Diercks, Y.-B. Zhang, N. Kornienko, E.M. Nichols, Y. Zhao, A.R. Paris, D. Kim, P. Yang, O.M. Yaghi, C.J. Chang, Covalent organic frameworks comprising cobalt porphyrins for catalytic CO_2 reduction in water, Science 349 (2015) 1208–1213.
[27] C.S. Diercks, S. Lin, N. Kornienko, E.A. Kapustin, E.M. Nichols, C. Zhu, Y. Zhao, C. J. Chang, O.M. Yaghi, Reticular electronic tuning of porphyrin active sites in covalent organic frameworks for electrocatalytic carbon dioxide reduction, J. Am. Chem. Soc. 140 (2018) 1116–1122.
[28] H. Dong, M. Lu, Y. Wang, H.-L. Tang, D. Wu, X. Sun, F.-M. Zhang, Covalently anchoring covalent organic framework on carbon nanotubes for highly efficient electrocatalytic CO_2 reduction, Appl. Catal. B: Environ. 303 (2022).
[29] Y.R. Wang, Q. Huang, C.T. He, Y. Chen, J. Liu, F.C. Shen, Y.Q. Lan, Oriented electron transmission in polyoxometalate-metalloporphyrin organic framework for highly selective electroreduction of CO_2, Nat. Commun. 9 (2018) 4466.
[30] H.J. Zhu, M. Lu, Y.R. Wang, S.J. Yao, M. Zhang, Y.H. Kan, J. Liu, Y. Chen, S.L. Li, Y. Q. Lan, Efficient electron transmission in covalent organic framework nanosheets for highly active electrocatalytic carbon dioxide reduction, Nat. Commun. 11 (2020) 497.
[31] S. An, C. Lu, Q. Xu, C. Lian, C. Peng, J. Hu, X. Zhuang, H. Liu, Constructing catalytic crown ether-based covalent organic frameworks for electroreduction of CO_2, ACS Energy Lett. 6 (2021) 3496–3502.
[32] Q. Wu, R.-K. Xie, M.-J. Mao, G.-L. Chai, J.-D. Yi, S.-S. Zhao, Y.-B. Huang, R. Cao, Integration of strong electron transporter tetrathiafulvalene into metalloporphyrin-based covalent organic framework for highly efficient electroreduction of CO_2, ACS Energy Lett. 5 (2020) 1005–1012.
[33] Q. Wu, M.J. Mao, Q.J. Wu, J. Liang, Y.B. Huang, R. Cao, Construction of donor-acceptor heterojunctions in covalent organic framework for enhanced CO_2 electroreduction, Small 17 (2021), e2004933.
[34] E.M. Johnson, R. Haiges, S.C. Marinescu, Covalent-organic frameworks composed of rhenium bipyridine and metal porphyrins: Designing Heterobimetallic frameworks with two distinct metal sites, ACS Appl. Mater. Interfaces 10 (2018) 37919–37927.
[35] Y. Lu, J. Zhang, W. Wei, D.D. Ma, X.T. Wu, Q.L. Zhu, Efficient carbon dioxide electroreduction over ultrathin covalent organic framework nanolayers with isolated cobalt porphyrin units, ACS Appl. Mater. Interfaces 12 (2020) 37986–37992.
[36] N. Huang, K.H. Lee, Y. Yue, X. Xu, S. Irle, Q. Jiang, D. Jiang, A stable and Conductive Metallophthalocyanine Framework for Electrocatalytic Carbon Dioxide Reduction in Water, Angew. Chem. Int. Ed. 59 (2020) 16587–16593.
[37] B. Han, X. Ding, B. Yu, H. Wu, W. Zhou, W. Liu, C. Wei, B. Chen, D. Qi, H. Wang, K. Wang, Y. Chen, B. Chen, J. Jiang, Two-dimensional covalent organic frameworks with Cobalt(II)-Phthalocyanine sites for efficient electrocatalytic carbon dioxide reduction, J. Am. Chem. Soc. 143 (2021) 7104–7113.
[38] G.C. Dubed Bandomo, S.S. Mondal, F. Franco, A. Bucci, V. Martin-Diaconescu, M. A. Ortuño, P.H. van Langevelde, A. Shafir, N. López, J. Lloret-Fillol, Mechanically constrained catalytic $Mn(CO)_3Br$ single sites in a two-dimensional covalent organic framework for CO_2 electroreduction in H_2O, ACS Catal. 11 (2021) 7210–7222.
[39] P.L. Cheung, S.K. Lee, C.P. Kubiak, Facile solvent-free synthesis of thin iron porphyrin cofs on carbon cloth electrodes for CO_2 reduction, Chem. Mater. 31 (2019) 1908–1919.
[40] Y.R. Wang, H.M. Ding, X.Y. Ma, M. Liu, Y.L. Yang, Y. Chen, S.L. Li, Y.Q. Lan, Imparting CO_2 electroreduction auxiliary for integrated morphology tuning and performance boosting in a porphyrin-based covalent organic framework, Angew. Chem. Int. Ed. (2021).
[41] P. Su, K. Iwase, T. Harada, K. Kamiya, S. Nakanishi, Covalent triazine framework modified with coordinatively-unsaturated Co or Ni atoms for CO_2 electrochemical reduction, Chem. Sci. 9 (2018) 3941–3947.
[42] J. Wu, R.M. Yadav, M. Liu, P.P. Sharma, C.S. Tiwary, L. Ma, X. Zou, X.-D. Zhou, B. I. Yakobson, J. Lou, P.M. Ajayan, Achieving highly efficient, selective, and stable CO_2 reduction on nitrogen-doped carbon nanotubes, ACS Nano 9 (2015) 5364–5371.
[43] C. Hu, Y. Xiao, Y. Zou, L. Dai, Carbon-based metal-free electrocatalysis for energy conversion, energy storage, and environmental protection, Electrochem. Energy Rev. 1 (2018) 84–112.
[44] X. Zhu, C. Tian, H. Wu, Y. He, L. He, H. Wang, X. Zhuang, H. Liu, C. Xia, S. Dai, Pyrolyzed triazine-based nanoporous frameworks enable electrochemical CO_2 reduction in water, ACS Appl. Mater. Interfaces 10 (2018) 43588–43594.
[45] Y. Wang, J. Chen, G. Wang, Y. Li, Z. Wen, Perfluorinated covalent triazine framework derived hybrids for the highly selective electroconversion of carbon dioxide into methane, Angew. Chem. Int. Ed. 57 (2018) 13120–13124.
[46] X. Suo, F. Zhang, Z. Yang, H. Chen, T. Wang, Z. Wang, T. Kobayashi, C.-L. Do-Thanh, D. Maltsev, Z. Liu, S. Dai, Highly perfluorinated covalent triazine frameworks derived from a low-temperature ionothermal approach towards enhanced CO_2 electroreduction, Angew. Chem. Int. Ed. 60 (2021) 25688–25694.
[47] A. Laemont, S. Abednatanzi, P.G. Derakshandeh, F. Verbruggen, E. Fiset, Q. Qin, K. Van Daele, M. Meledina, J. Schmidt, M. Oschatz, P. Van Der Voort, K. Rabaey, M. Antonietti, T. Breugelmans, K. Leus, Covalent triazine framework/carbon nanotube hybrids enabling selective reduction of CO_2 to CO at low overpotential, Green. Chem. 22 (2020) 3095–3103.
[48] C. Lu, J. Yang, S. Wei, S. Bi, Y. Xia, M. Chen, Y. Hou, M. Qiu, C. Yuan, Y. Su, F. Zhang, H. Liang, X. Zhuang, Atomic Ni anchored covalent triazine framework as high efficient electrocatalyst for carbon dioxide conversion, Adv. Funct. Mater. 29 (2019).
[49] D.A. Popov, J.M. Luna, N.M. Orchanian, R. Haiges, C.A. Downes, S.C. Marinescu, A 2,2′-Bipyridine-containing covalent organic framework bearing Rhenium(I) tricarbonyl moieties for CO_2 reduction, Dalton Trans. 47 (2018) 17450–17460.
[50] M. Lu, Q. Li, J. Liu, F.-M. Zhang, L. Zhang, J.-L. Wang, Z.-H. Kang, Y.-Q. Lan, Installing earth-abundant metal active centers to covalent organic frameworks for efficient heterogeneous photocatalytic CO_2 reduction, Appl. Catal. B: Environ. 254 (2019) 624–633.
[51] R.K. Yadav, A. Kumar, N.-J. Park, K.-J. Kong, J.-O. Baeg, A highly efficient covalent organic framework film photocatalyst for selective solar fuel production from CO_2, J. Mater. Chem. A 4 (2016) 9413–9418.
[52] Y. Fu, X. Zhu, L. Huang, X. Zhang, F. Zhang, W. Zhu, Azine-based covalent organic frameworks as metal-free visible light photocatalysts for CO_2 reduction with H_2O, Appl. Catal. B: Environ. 239 (2018) 46–51.
[53] K. Lei, D. Wang, L. Ye, M. Kou, Y. Deng, Z. Ma, L. Wang, Y. Kong, A. Metal-Free, Donor-acceptor covalent organic framework photocatalyst for visible-light-driven reduction of CO_2 with H_2O, ChemSusChem 13 (2020) 1725–1729.
[54] J.-X. Cui, L.-J. Wang, L. Feng, B. Meng, Z.-Y. Zhou, Z.-M. Su, K. Wang, S. Liu, A metal-free covalent organic framework as a photocatalyst for CO_2 reduction at low CO_2 concentration in a gas–solid system, J. Mater. Chem. A 9 (2021) 24895–24902.
[55] L. Peng, S. Chang, Z. Liu, Y. Fu, R. Ma, X. Lu, F. Zhang, W. Zhu, L. Kong, M. Fan, Visible-light-driven photocatalytic CO_2 reduction over ketoenamine-based covalent organic frameworks: Role of the host functional groups, Catal. Sci. Technol. 11 (2021) 1717–1724.
[56] S. Yang, W. Hu, X. Zhang, P. He, B. Pattengale, C. Liu, M. Cendejas, I. Hermans, X. Zhang, J. Zhang, J. Huang, 2D covalent organic frameworks as intrinsic photocatalysts for visible light-driven CO_2 reduction, J. Am. Chem. Soc. 140 (2018) 14614–14618.
[57] D. Wang, D. Streater, Y. Peng, J. Huang, 2D covalent organic frameworks with an incorporated manganese complex for light driven carbon dioxide reduction, ChemPhotoChem 5 (2021) 1119–1123.
[58] S.-Y. Li, S. Meng, X. Zou, M. El-Roz, I. Telegeev, O. Thili, T.X. Liu, G. Zhu, Rhenium-functionalized covalent organic framework photocatalyst for efficient CO_2 reduction under visible light, Microporous Mesoporous Mater. 285 (2019) 195–201.
[59] Z. Fu, X. Wang, A.M. Gardner, X. Wang, S.Y. Chong, G. Neri, A.J. Cowan, L. Liu, X. Li, A. Vogel, R. Clowes, M. Bilton, L. Chen, R.S. Sprick, A.I. Cooper, A stable covalent organic framework for photocatalytic carbon dioxide reduction, Chem. Sci. 11 (2020) 543–550.
[60] W. Zhong, R. Sa, L. Li, Y. He, L. Li, J. Bi, Z. Zhuang, Y. Yu, Z. Zou, A covalent organic framework bearing single Ni sites as a synergistic photocatalyst for selective photoreduction of CO_2 to CO, J. Am. Chem. Soc. 141 (2019) 7615–7621.
[61] S. Yang, R. Sa, H. Zhong, H. Lv, D. Yuan, R. Wang, Microenvironments enabled by covalent organic framework linkages for modulating active metal species in photocatalytic CO_2 reduction, Adv. Funct. Mater. (2022).
[62] Y.N. Gong, W. Zhong, Y. Li, Y. Qiu, L. Zheng, J. Jiang, H.L. Jiang, Regulating photocatalysis by spin-state manipulation of cobalt in covalent organic frameworks, J. Am. Chem. Soc. 142 (2020) 16723–16731.
[63] M. Lu, J. Liu, Q. Li, M. Zhang, M. Liu, J.L. Wang, D.Q. Yuan, Y.Q. Lan, Rational design of crystalline covalent organic frameworks for efficient CO_2 photoreduction with H_2O, Angew. Chem. Int. Ed. 58 (2019) 12392–12397.
[64] T. Skorjanc, D. Shetty, M.E. Mahmoud, F. Gandara, J.I. Martinez, A.K. Mohammed, S. Boutros, A. Merhi, E.O. Shehayeb, C.A. Sharabati, P. Damacet, J. Raya, S. Gardonio, M. Hmadeh, B.R. Kaafarani, A. Trabolsi, Metallated isoindigo-porphyrin covalent organic framework photocatalyst with a narrow band gap for efficient CO_2 conversion, ACS Appl. Mater. Interfaces 14 (2022) 2015–2022.
[65] P. Sarkar, S. Riyajuddin, A. Das, A. Hazra Chowdhury, K. Ghosh, S.M. Islam, Mesoporous covalent organic framework: An active photo-catalyst for formic acid synthesis through carbon dioxide reduction under visible light, Mol. Catal. 484 (2020).
[66] W. Liu, X. Li, C. Wang, H. Pan, W. Liu, K. Wang, Q. Zeng, R. Wang, J. Jiang, A scalable general synthetic approach toward ultrathin imine-linked two-dimensional covalent organic framework nanosheets for photocatalytic CO_2 reduction, J. Am. Chem. Soc. 141 (2019) 17431–17440.
[67] Z. Liu, Y. Huang, S. Chang, X. Zhu, Y. Fu, R. Ma, X. Lu, F. Zhang, W. Zhu, M. Fan, Highly dispersed Ru nanoparticles on a bipyridine-linked covalent organic framework for efficient photocatalytic CO_2 Reduction, Sustain. Energy Fuels 5 (2021) 2871–2876.
[68] L. Wang, G. Huang, L. Zhang, R. Lian, J. Huang, H. She, C. Liu, Q. Wang, Construction of TiO_2-covalent organic framework Z-scheme hybrid through coordination bond for photocatalytic CO_2 conversion, J. Energy Chem. 64 (2022) 85–92.
[69] M. Zhang, M. Lu, Z.L. Lang, J. Liu, M. Liu, J.N. Chang, L.Y. Li, L.J. Shang, M. Wang, S.L. Li, Y.Q. Lan, Semiconductor/Covalent-organic-framework Z-Scheme heterojunctions for artificial photosynthesis, Angew. Chem. Int. Ed. 59 (2020) 6500–6506.

[70] H. Zhong, R. Sa, H. Lv, S. Yang, D. Yuan, X. Wang, R. Wang, Covalent organic framework hosting metalloporphyrin-based carbon dots for visible-light-driven selective CO_2 reduction, Adv. Funct. Mater. 30 (2020).

[71] J. Li, P. Liu, H. Huang, Y. Li, Y. Tang, D. Mei, C. Zhong, Metal-Free 2D/2D black phosphorus and covalent triazine framework heterostructure for CO_2 photoreduction, ACS Sustain. Chem. Eng. 8 (2020) 5175–5183.

[72] Z. Zhao, D. Zheng, M. Guo, J. Yu, S. Zhang, Z. Zhang, Y. Chen, Engineering olefin-linked covalent organic frameworks for photoenzymatic reduction of CO_2, Angew. Chem. Int. Ed. (2022).